FINAL REPORT FOR

ONR GRANT NO. N00014-90-J-4095

"STUDIES OF UPCONVERSION LASERS"

Prepared for

Dr. L. N. Durvasula
DARPA/DSO
3701 N. Fairfax Dr.
Arlington, VA 22203-1714

Prepared by

J. G. Eden
University of Illinois
Department of Electrical and Computer Engineering
1406 West Green Street
Urbana, IL 61801

October 1996

I. INTRODUCTION

The thrust of this research program was the development of new, compact sources of visible and ultraviolet (UV) radiation based on upconversion in rare earth-doped crystals and glass fibers. Several applications in medical diagnostics, reprographics and displays, in particular, require reliable (preferably solid state), room temperature sources of low power ($\lesssim$ 1 W), CW radiation that have not, until recently, existed.

This research program proved to be extremely fruitful. Specifically, these experiments pursued rare earth-doped fluorozirconate glass (ZBLAN) fibers as the host for new visible and UV oscillators and the following major developments were achieved:

- The first UV fiber laser (pumped by any means) was demonstrated; this laser is also the shortest wavelength glass laser;
- The first violet fiber laser (λ = 413 nm) was demonstrated;
- Single line operation of the Ho:ZBLAN fiber laser was achieved and a power output exceeding 35 mW was obtained.

In addition to these results, advances in the technology of upconversion fiber lasers, such as reduced pump power thresholds and improved approaches for preparing the ends of ZBLAN fibers for oscillator experiments, were realized during the course of this work.

This report will summarize the highlights of the results obtained in this program. Details concerning the experiments and the operation of the fiber lasers can be found in the reprints in Appendix A.

II. EXPERIMENTAL RESULTS

A. Rare Earth-Doped Crystals: Er:YLF, BaY_2F_8

In the early phases of this program, our efforts focused on rare earth-doped fluoride crystals because of the availability of high optical quality samples and the large rare earth doping concentrations (> 5 at. %) that are readily obtainable in bulk crystals. Both our experimental and theoretical efforts focused on Er-doped crystals and experiments entailed measurements of both absorption and emission spectra. Figure 1 shows the absorption spectrum of an Er:$LiYF_4$ crystal at 300 K in the near-ultraviolet and visible. The Er concentration is 5 at. % and note the presence of several potential pumping bands. Transitions terminating on the $^4I_{9/2,\ 11/2,\ 13/2}$ states of Er^{3+} lie further to the near-IR and Fig. 2 shows details of the $^4I_{11/2} \leftarrow {}^4I_{15/2}$ absorption spectrum of Er^{3+} that was recorded at room temperature with a flashlamp source. Analysis of the band resulted in assignments for each of the features to transitions between specific Stark sublevels of the $^4I_{11/2}$ and $^4I_{15/2}$ manifolds.

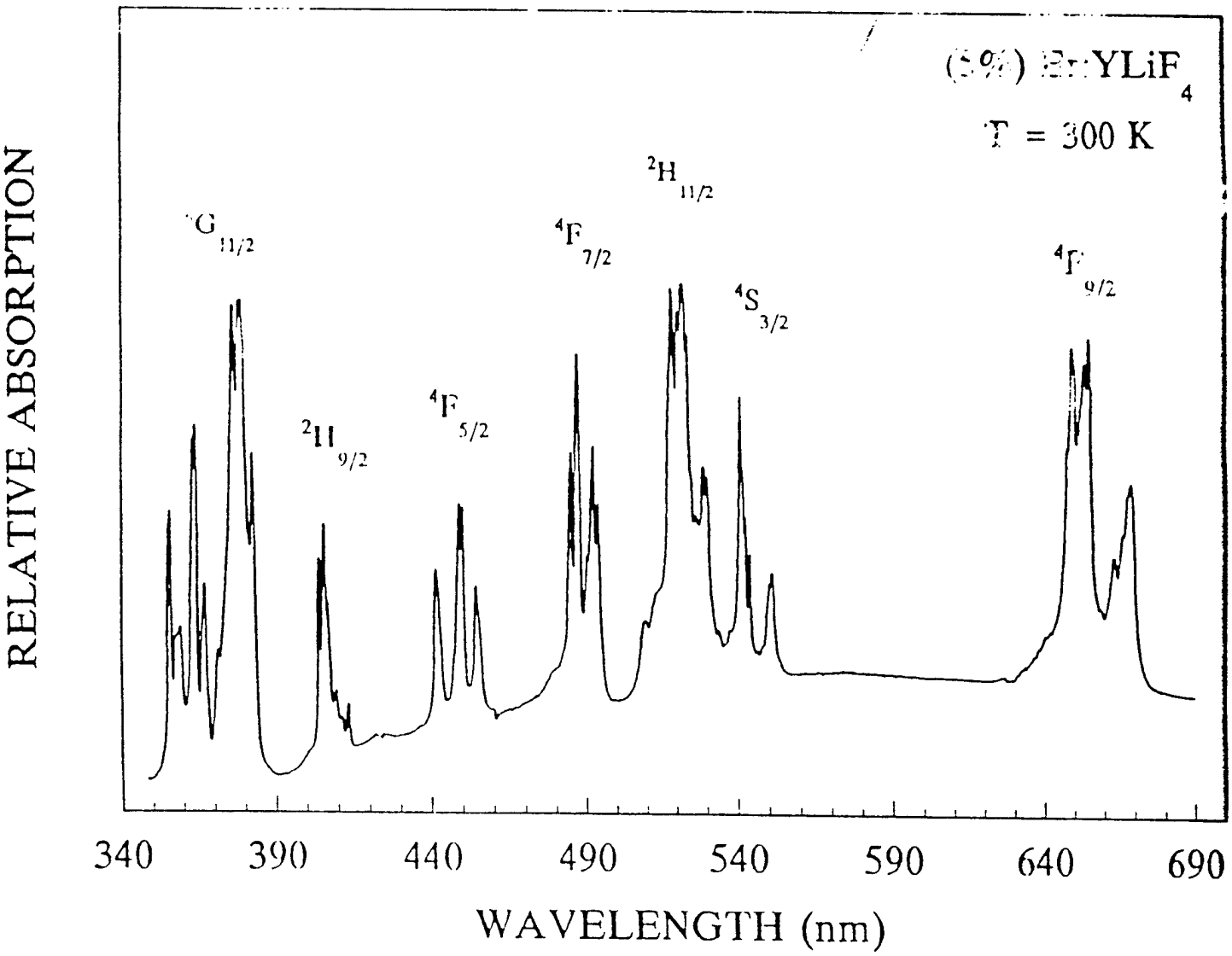

Fig. 1 Absorption of an Er(5 at.%)-doped $YLiF_4$ crystal at room temperature in the near-UV and visible.

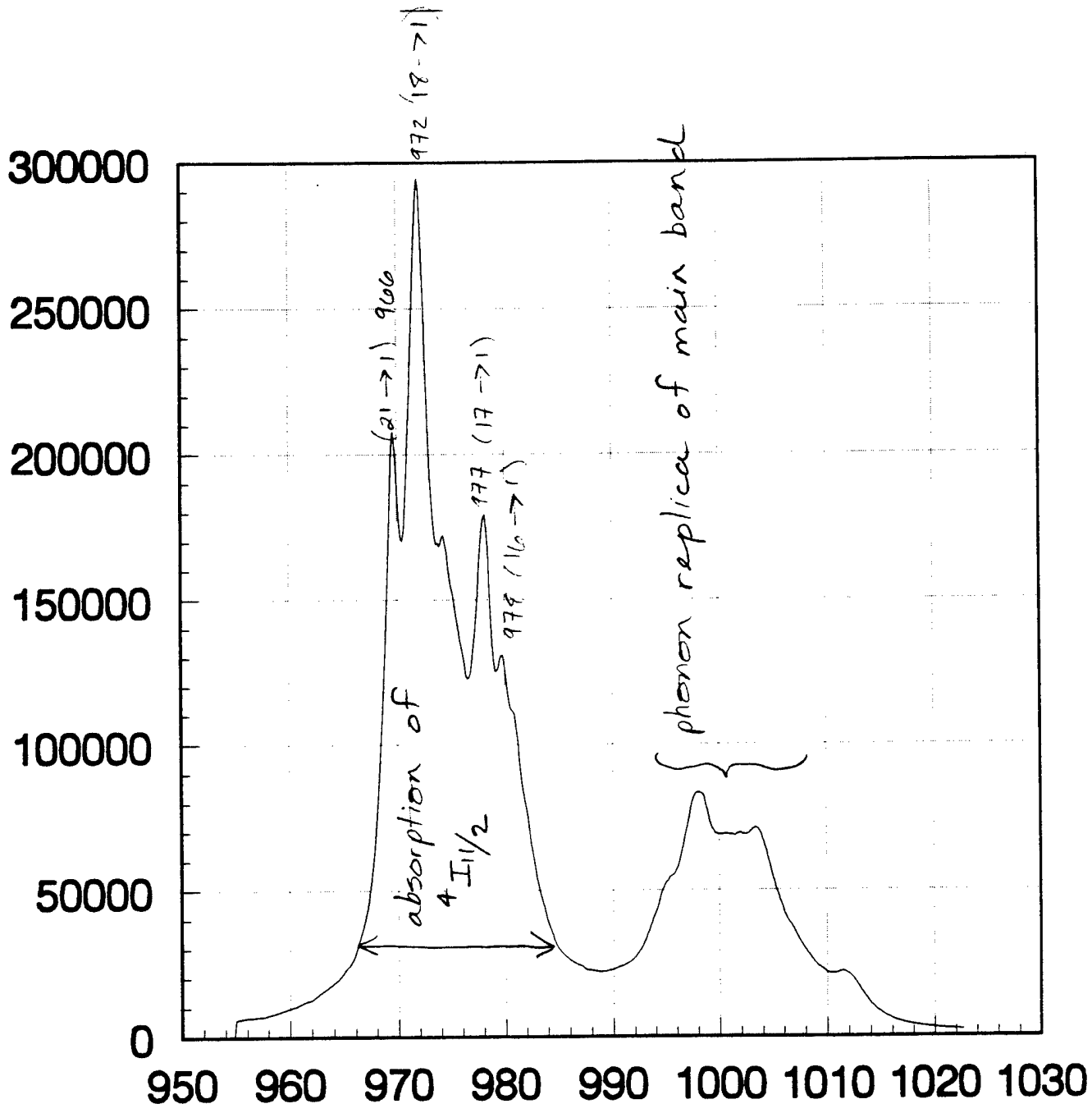

Fig. 2 Absorption spectrum of Er:YLF ($LiYF_4$) in the near-IR showing details of the $^4I_{11/2} \leftarrow {}^4I_{15/2}$ transition of Er^{3+}.

A systematic study of Er-doped $LiYF_4$ and BaY_2F_8 bulk crystals was carried out in an effort to identify the optimal rare earth ion transitions for a diode laser-pumped upconversion laser. Figure 3 illustrates the pumping pathways and dominant emission lines when Er:$LiYF_4$ (YLF) is pumped in the red ($\lambda \sim 650$ nm, $^4F_{9/2} \leftarrow {}^4I_{15/2}$). Because of the excitation scheme, and the upper state lifetimes for Er^{3+} levels in the 18,000–26,000 cm^{-1} region, strongest fluorescence occurs on the $^4S_{3/2} \rightarrow$ ground ($^4I_{15/2}$) transition in the green (551 nm) with weaker emission observed at 413 nm in the violet. The fluorescence spectrum of an Er (10 at.%):YLF crystal in the 350-600 nm region when pumped at 653 nm is shown in Fig. 4. Green emission dominates spectra taken at both room temperature and 77 K but the violet line intensifies dramatically when the crystal is cooled. This suggests that the strongest violet line originates from one of the low-lying states of the $^2H_{9/2}$ Stark minifold of Er^{3+}. The importance of the Er^{3+} concentration to the upconversion process is illustrated by the violet spectra of Fig. 5 which were recorded for Er^{3+} doping levels of 1, 5, and 10 at.% in YLF. The spectra, acquired at 77 K, show a rapid rise in intensity as [Er^{3+}] is increased, accompanied by narrowing of the strongest feature at ~413 nm. These results are representative of those obtained for the green transition and suggest that, at least for Er^{3+} concentrations up to 10 at.%, increasing the rare earth ion number density is advantageous to upconversion. Similar data were obtained when pumping an Er (5 at.%):YLF crystal at 800 nm ($^4I_{9/2} \leftarrow {}^4I_{15/2}$) and Fig. 6 presents representative spectra that were obtained in the violet and green. Temperatures as low as 15 K were studied.

In addition to a thorough study of the optical properties of Er:YLF crystals as a function of pumping wavelength, Er^{3+} concentration, and temperature, several experiments were conducted to compare $LiYF_4$ (YLF) with BaY_2F_8 as a host. The phonon spectrum for the latter crystal lies lower in energy than that for $LiYF_4$ and, indeed, experimental observations demonstrate that BaY_2F_8 is a more attractive host for an upconversion laser. A comparison of the emission spectra for Er:$LiYF_4$ and Er:BaY_2F_8 crystals in the violet and green when pumped at 653 nm is given in Fig. 7. Although the Er number densities in the two crystals differ by almost two orders of magnitude, the green emission from the doped BaY_2F_8 is extremely intense and is clearly the more efficient host. Our studies strongly suggest that future studies of rare earth upconversion lasers in crystals should focus on BaY_2F_8.

In parallel with the experimental effort, a theoretical program was conducted for the purpose of guiding the experiments. For example, multiplet branching ratios for different Er^{3+} radiating states were calculated for Er^{3+}: YLF crystals. For the $^2H_{9/2}$ state, the branching ratio for the 413 nm transition is 57% whereas the next largest one is 35% for the $^2H_{9/2} \rightarrow {}^4I_{13/2}$ transitions. Similarly, the branching ratio for the $^5S_2 \rightarrow {}^5I_8$ transition (at 551 nm) for Ho^{3+} in BaY_2F_8 was determined to be 54%. To analyze the low temperature data, similar calculations were carried out for the Stark sublevels of the upper and lower states. That is, branching ratios

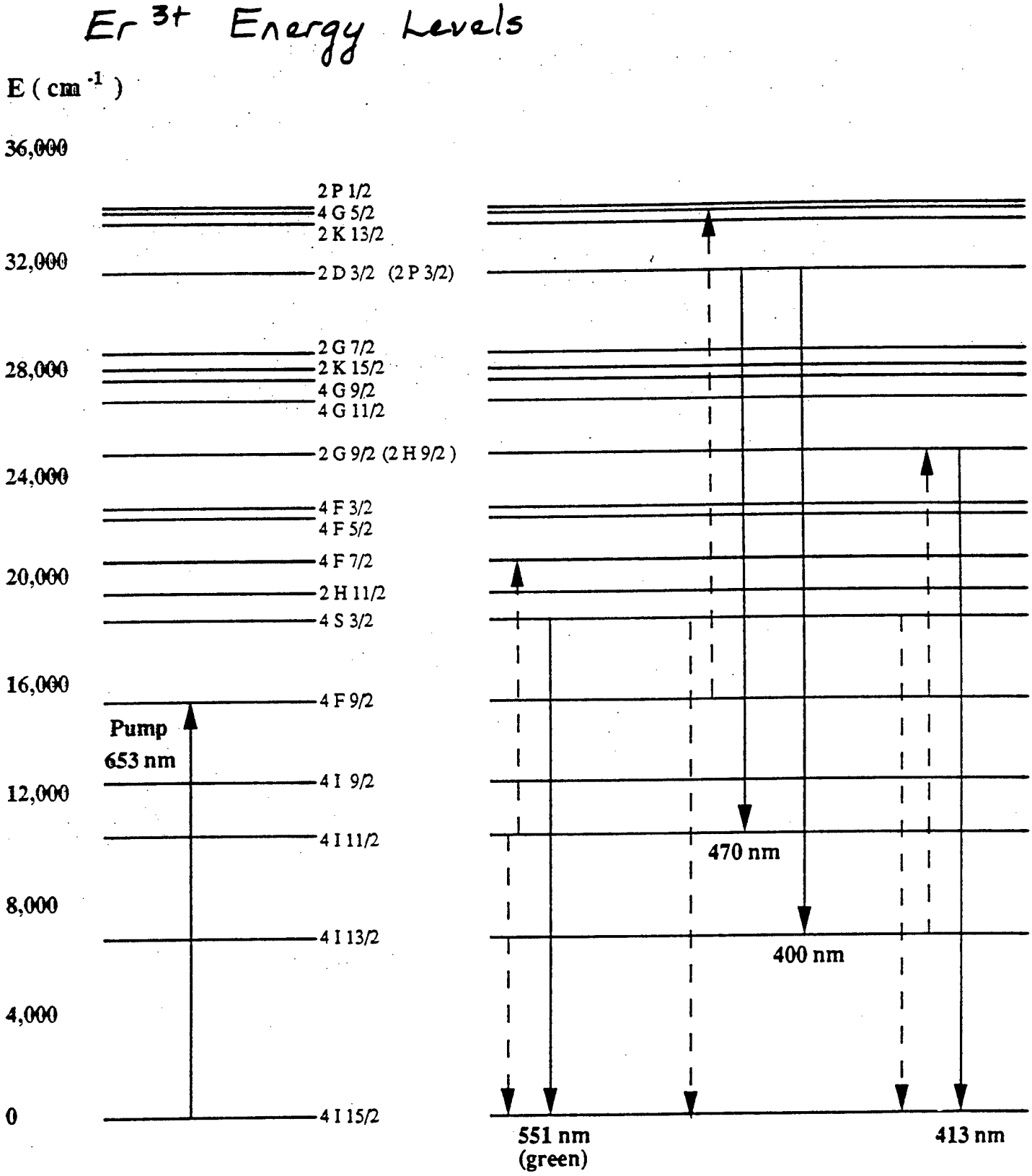

Fig. 3 Partial energy level diagram of Er^{3+} in YLF.

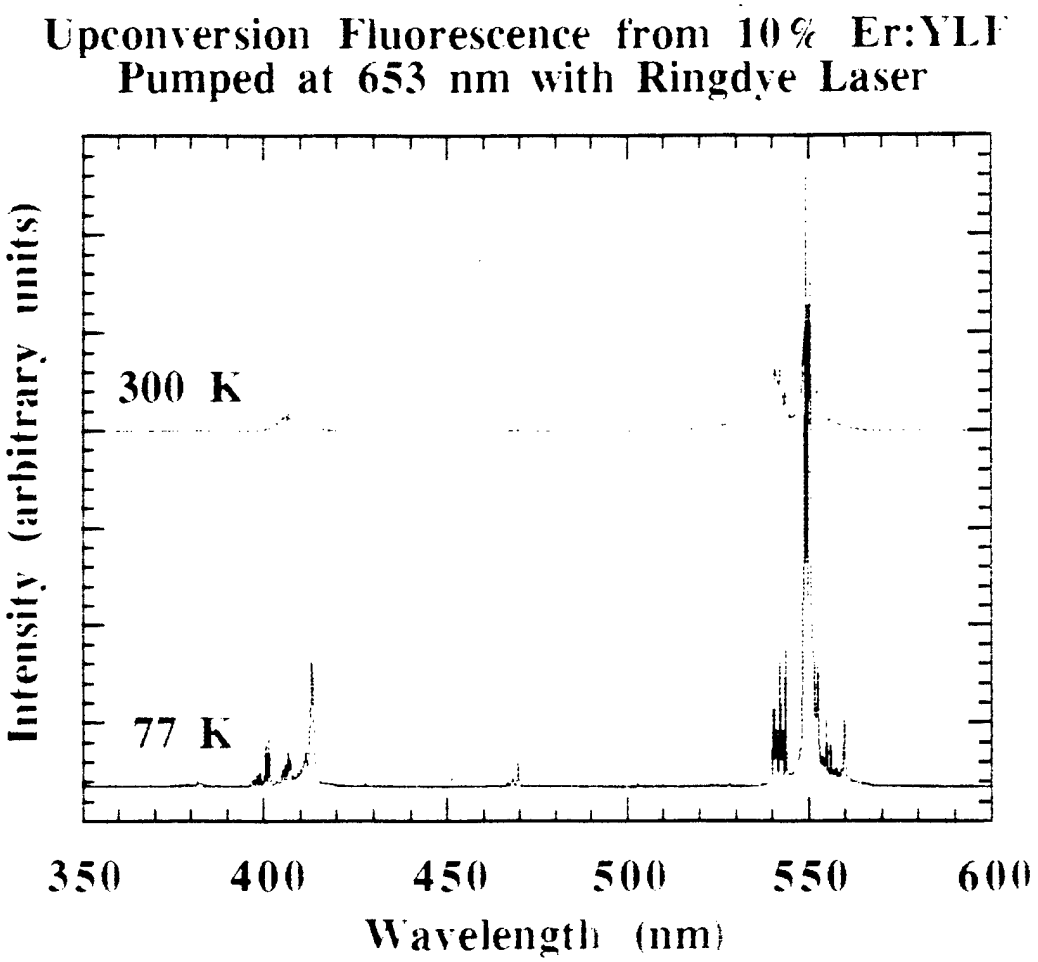

Fig. 4 Emission spectrum of Er(10 at. %):YLF in the 350-600 nm region at 77 and 300 K. The crystal was excited at 653 nm.

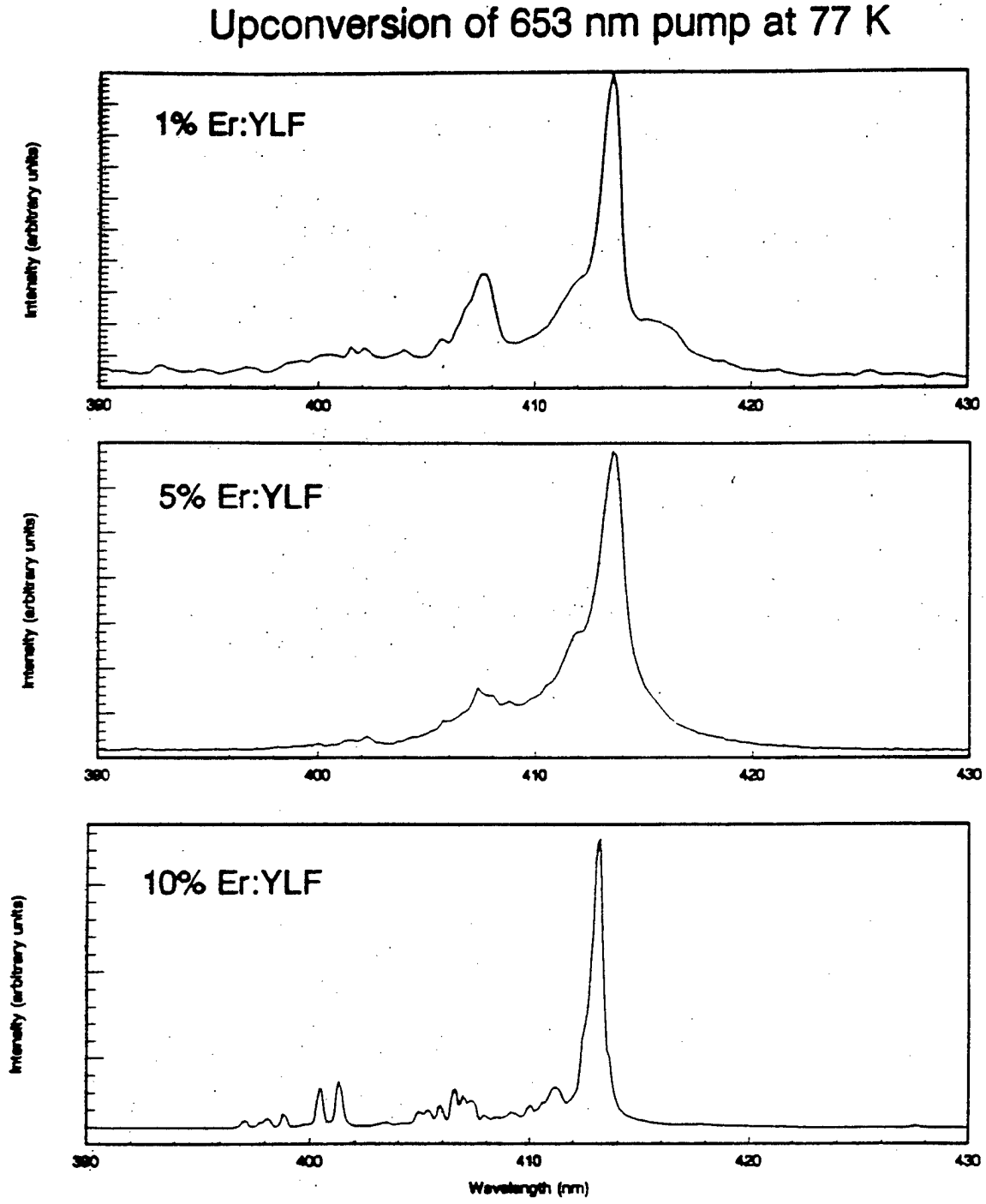

Fig. 5 Dependence of Er^{3+} violet (413 nm) emission in Er:YLF crystals on the Er^{3+} concentration. For clarity, all three spectra have been normalized in intensity.

Upconversion of 800 nm Pump in (5%) Er:YLF

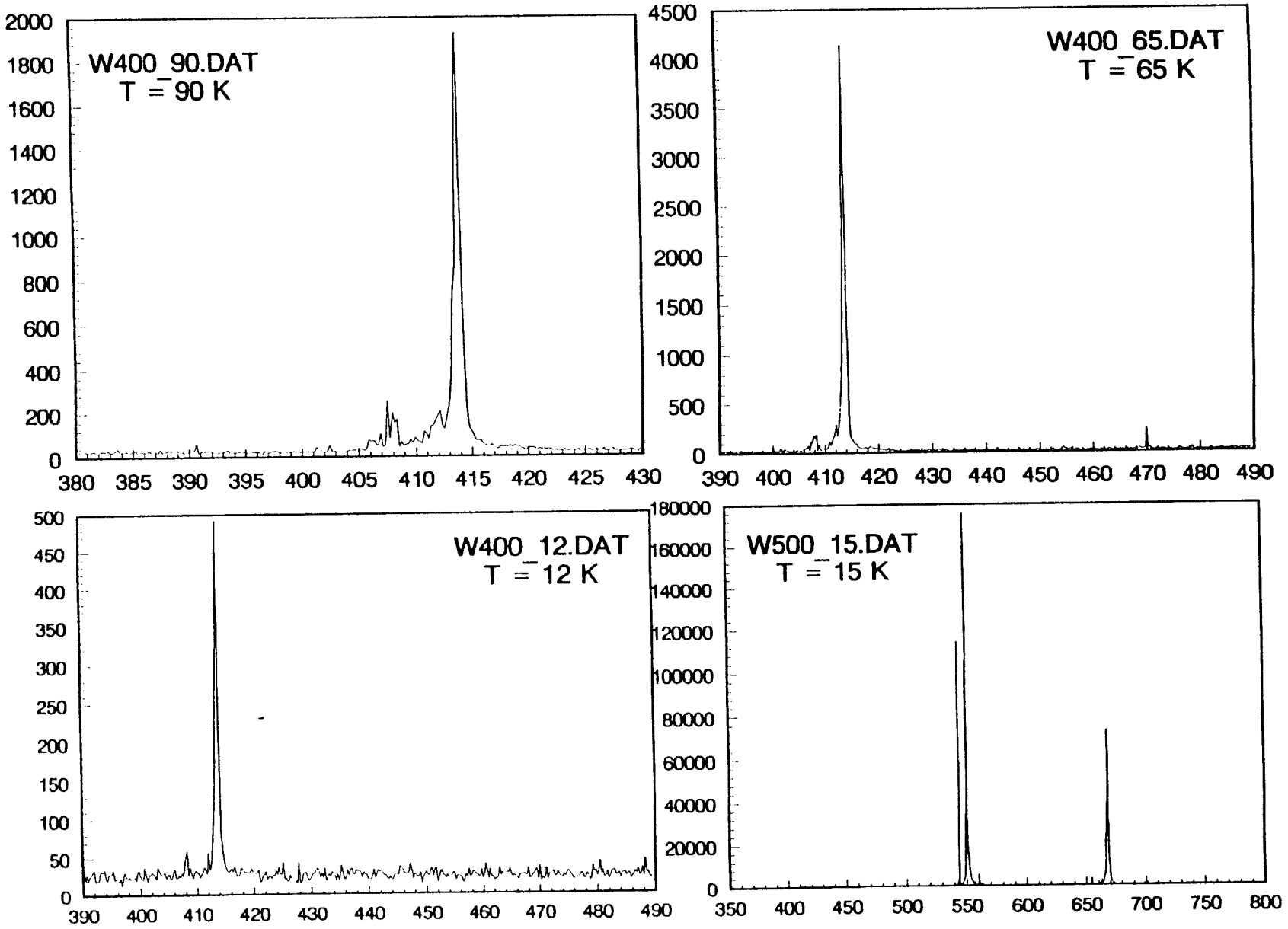

Fig. 6 Emission spectra in the violet and green for an Er (5 at. %):YLF crystal excited via the $^4I_{9/2} \leftarrow {}^4I_{15/2}$ transition at 800 nm.

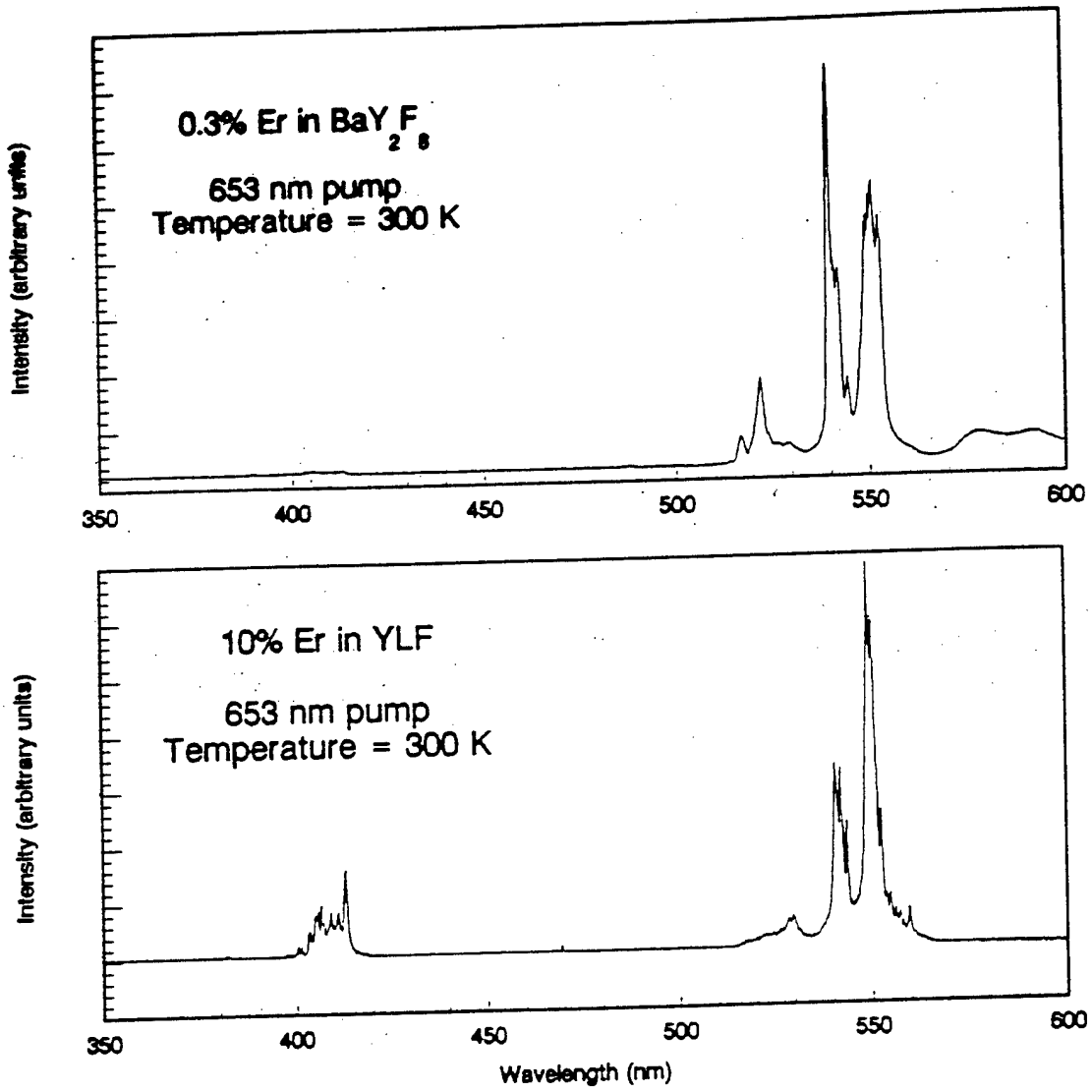

Fig. 7 Comparison of the emission spectra for Er:BaY_2F_8 (top) and Er:$LiYF_4$ crystals in the 350-600 nm region. Note that the Er concentrations differ by almost two orders of magnitude.

were calculated for transitions between specific Stark sublevels of the upper and lower Er^{3+} states. Finally, it should be mentioned that the upconversion constant, α, was calculated for Er:YLF for several Er doping levels. For 10 at.% of Er, for example, α was calculated for the $^4I_{11/2}$ multiplet of Er^{3+} to be $1.04 \cdot 10^{-17}$ cm^3–sec^{-1} whereas the experimental value reported by Chou and Jenssen (1989) is $1.8 \cdot 10^{-17}$ cm^3–sec^{-1}. At higher doping levels, the agreement between experiment and theory is better. For [Er] = 30 at.%, the experimental and theoretical values for α are $3.0 \cdot 10^{-17}$ and $3.1 \cdot 10^{-17}$ cm^3–s^{-1}, respectively.

B. Ho:ZBLAN Fiber Laser

Although the experimental and computational program described in the preceding section was valuable in identifying the optimal conditions for demonstrating a rare earth upconversion laser in bulk crystals, several attempts to produce stimulated emission made it clear that an efficient laser in a bulk crystal would not be possible unless the pump beam could be confined spatially in a waveguide. That is, the upconversion pumping rate is sensitive to pump intensity and, in the absence of a waveguide, the pumping intensity will not be maintained throughout the crystal.

For this reason, once rare earth-doped fluoride glass fibers became available soon after the start of this program, we focused our efforts on demonstrating and optimizing upconversion fiber lasers. This work proved to be extremely fruitful. Lasing was observed almost immediately in Ho-doped fluorozirconate glass (ZBLAN) fibers and Fig. 8 shows one of the first laser spectra obtained under this program. Emission from a free-running oscillator occurs predominantly on a single line at λ ~549 nm and subsequent work showed that the pump wavelength could be tuned over a 10 nm region in the red! Extensive output coupling data were obtained for this fiber laser and representative data are presented in Fig. 9. These early results yielded 12 mW of output power for 5% output coupling. Later, we obtained more than 35 mW of output power at a slope efficiency of 24% when the cavity output coupling is 30%. Furthermore, dramatic reductions in the threshold pumping power of this laser have been realized as a result of this program. As a result of considerable improvements in fiber preparation, optical inspection and mirror mounting, threshold powers have dropped by more than an order of magnitude (hundreds of mW $\rightarrow$ tens of mW) and are now well within the realm of pumping by semiconductor diodes. Also, we were successful in tuning this laser over more than 10 nm in the green and the reprints in the Appendix describe in detail the performance of the laser.

In addition to the exciting results obtained with the green fiber laser, the senior graduate student on this program (David Funk) was able to obtain stimulated emission from an Nd:ZBLAN fiber in the violet (413 nm) and near-UV (381 nm). Not only are these wavelengths

Ho:ZBLAN FIBER LASER

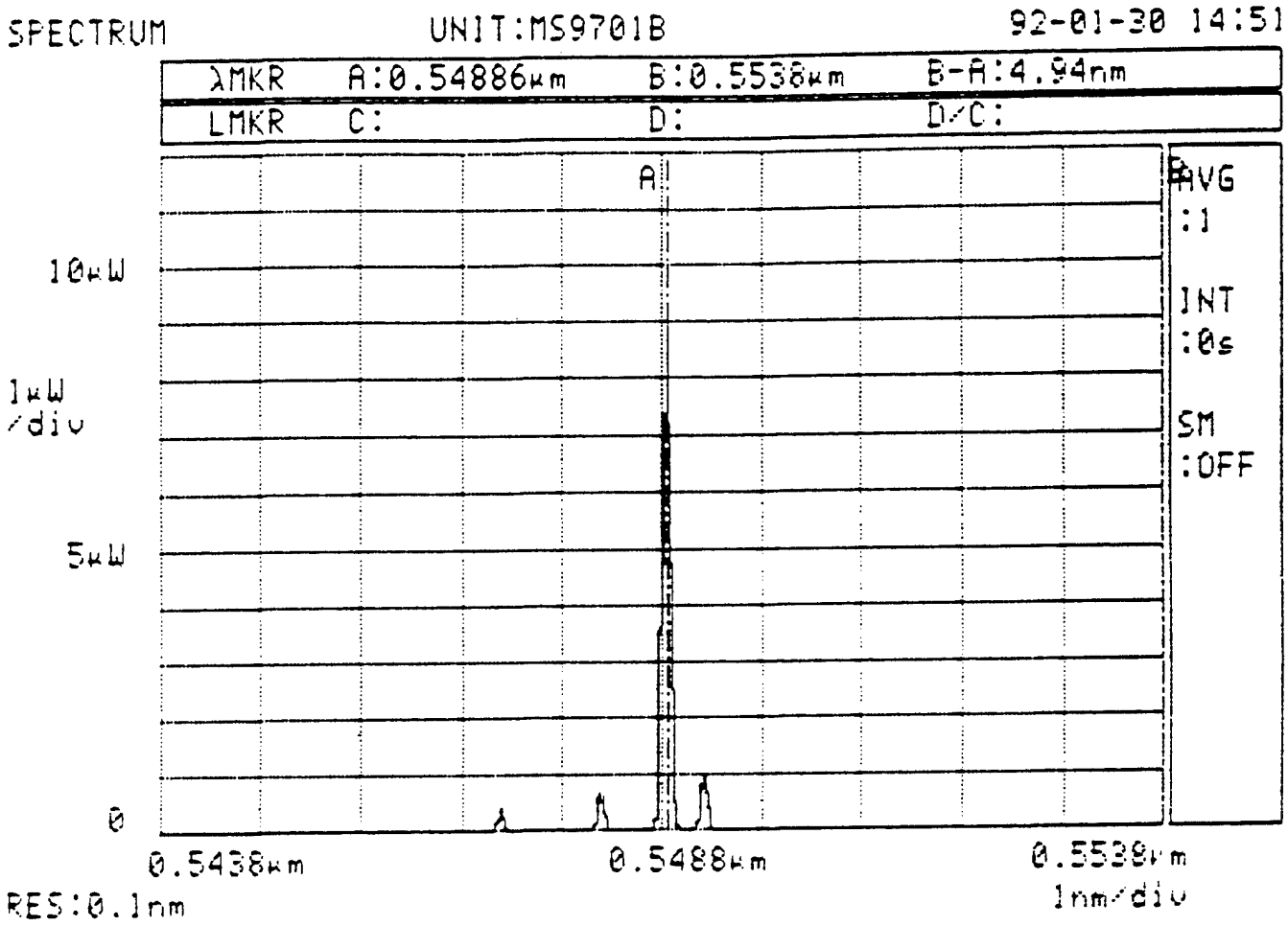

PUMP TUNING RANGE: > 10 nm!

Fig. 8 Laser spectrum recorded for a Ho:ZBLAN fiber. This was one of the first such spectra obtained under this program.

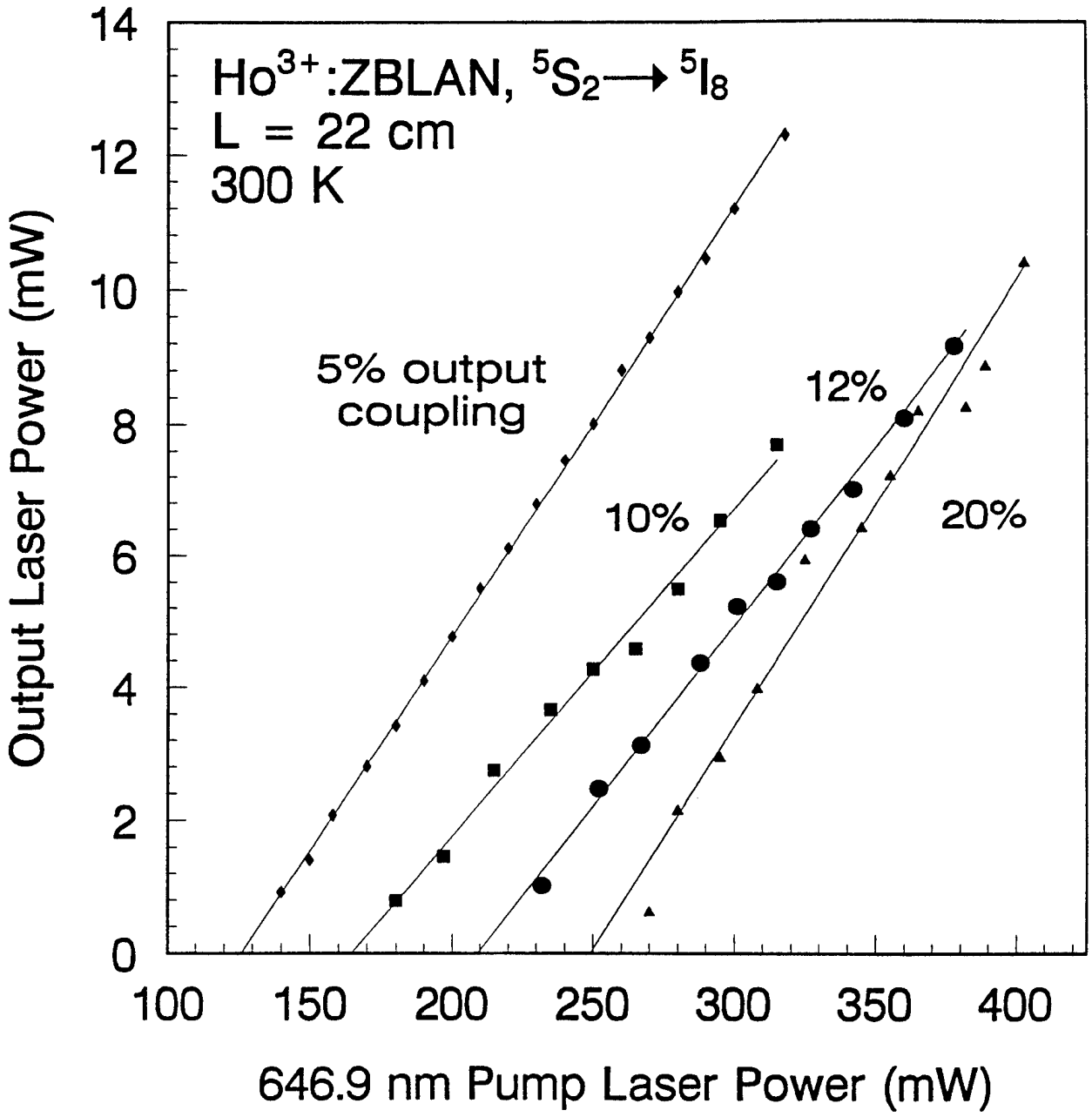

Fig. 9 Early output power measurements for an NA = 0.2 fiber (Ho:ZBLAN, 1000 ppm Ho), 22 cm in length. Maximum output powers of 12 mW were obtained.

the shortest obtained from an upconversion fiber, but the latter represents the first UV fiber laser pumped by any means and the first glass laser in the UV. To date, the output powers obtained on these transitions are modest: > 70 μW in the UV and ~500 μW in the violet but cavity output coupling and fiber length have not yet been optimized. The potential applications for this laser in medical diagnostics, reprographics and sensing are enormous and we are convinced that major improvements in laser performance will be realized with attention given to fiber composition and fabrication.

III. SUMMARY

The motivation behind this program at its inception was the development of efficient upconversion lasers in rare earth-doped materials. We believe that this research effort was quite successful as it resulted in a highly efficient Ho fiber laser in the green and the demonstration of the first ultraviolet fiber laser.

In closing, we wish to express our thanks to DARPA and, in particular, to Dr. L. N. Durvasula for the support of this program.

PAPERS PUBLISHED UNDER DARPA SUPPORT

1. D. S. Funk, S. B. Stevens, and J. G. Eden, "Excitation spectra of the green Ho: Fluorozirconate glass fiber laser," *IEEE Photon. Tech. Lett.* **5**, pp. 154-157 (1993).
2. D. S. Funk, J. W. Carlson, and J. G. Eden, "Ultraviolet (381 nm), room temperature laser in neodymium-doped fluorozirconate fiber," *Electron. Lett.* **30**, pp. 1859-1860 (1994).
3. D. S. Funk, J. W. Carlson, and J. G. Eden, "Room temperature fluorozirconate glass fiber laser in the violet (412 nm)," *Opt. Lett.* **20**, pp. 1474-1476 (1995).
4. D. S. Funk and J. G. Eden, "Glass fiber lasers in the ultraviolet and visible," *IEEE J. Sel. Topics Quant. Electron.* **1**, pp. 784-791 (1995).
5. D. S. Funk, S. B. Stevens, S. S. Wu, and J. G. Eden, "Tuning, temporal, and spectral characteristics of the green (λ ~549 nm), holmium-doped fluorozirconate glass fiber laser," *IEEE J. Quant. Electron.* **32**, pp. 638-645 (1996).
6. D. S. Funk and J. G. Eden, "Upconversion fiber lasers operating in the visible and ultraviolet," (to be published in Proc. SPIE).

APPENDIX:

SELECTED REPRINTS

PTL/5/2//06431

Excitation Spectra of the Green Ho: Fluorozirconate Glass Fiber Laser

D. S. Funk
S. B. Stevens
J. G. Eden

Reprinted from
IEEE PHOTONICS TECHNOLOGY LETTERS
Vol. 5, No. 2, February 1993

Excitation Spectra of the Green Ho: Fluorozirconate Glass Fiber Laser

D. S. Funk, S. B. Stevens, and J. G. Eden

Abstract—**Laser and fluorescence excitation spectra of the green Ho:ZBLAN glass fiber laser ($^5S_2 \rightarrow {}^5I_8$:546.9-550.1 nm) have been measured at room temperature by pumping 20–90 cm long fibers in the 640-653 nm spectral region ($^5F_5 \leftarrow {}^5I_8$ transition of Ho^{3+}) with a CW dye laser. Pronounced structure in the laser excitation spectrum appears to arise from Stark sublevels of the Ho^{3+} $^5F_5$ and $^5I_8$ states rather than excited state absorption. Because the overall gain profile is inhomogeneously broadened, the laser excitation spectrum width increases with pump power and is ~5.7 nm FWHM when the pump power is a factor of 2.3 above threshold. For a 22 cm fiber, the threshold pump power is 128 ± 5 mW and, with 5% output coupling, more than 12 mW has been extracted in the green for 318 mW of 646.7 nm input power. The slope efficiency for this oscillator (accounting for the pump launch efficiency) exceeds 14%.**

BULK $LiYF_4$ and BaY_2F_8 crystals have proven attractive as hosts for rare earth upconversion lasers, largely because their low average phonon frequencies reduce nonradiative (multiphonon) losses from excited states of the rare earth ion. However, the lengths of available crystals are presently restricted to, at most, a few centimeters, and the two-step pumping process inherent to upconversion lasers generally demands that the pump intensity and pump/gain medium interaction length be maximized.

Fibers drawn from fluorozirconate glass (ZBLAN) also offer a favorable phonon spectrum (cutoff < 600 cm^{-1}), provide a convenient means for confining the pump beam, and yet are available in lengths exceeding 1 m. Within the past three years, stimulated emission in the visible from Tm, Ho, Er and Pr-doped ZBLAN fibers has been reported [1]–[8]. Among these lasers, Ho has thus far exhibited the highest photon conversion efficiency. Other attractive characteristics are its broad tunability, ability to operate at room temperature and the need for only a single pump wavelength. By pumping a 2.7 μm diameter core Ho:ZBLAN fiber of optimized length (45 cm) at ~647.1 nm ($^5F_5 \leftarrow {}^5I_8$ transition), Allain, Monerie and Poignant [2], [3] obtained 11 mW of output power at 550 nm for an overall energy conversion efficiency of 3.6% but a slope efficiency (with respect to the launched pump power) of 36%.

Further improvement of the upconversion fiber lasers will undoubtedly be coupled to a better understanding of the channels by which energy flows from the state(s) initially pumped by the optical source to the upper laser level. Toward that end, this letter describes the measurement and implications of laser excitation spectra (i.e., dependence of output power on pump wavelength) for the green ($\lambda \sim 550$ nm) Ho:ZBLAN fiber laser. Comparisons of the *laser* and *fluorescence* excitation spectra recorded for several Ho^{3+} excited states suggest that the structure observed in both types of spectra is attributable to Stark levels of the $^5F_5$ and $^5I_8$ states rather than excited state absorption or mode coupling effects in the fiber. Other characteristics of this laser, including variations in the laser spectrum observed upon tuning the pumping wavelength and the dependence of threshold and slope efficiency on cavity output coupling, will also be discussed.

The fibers used in these experiments were fabricated from ZBLAN glass doped with 1000 ppm (by weight) of holmium; the diameters of the core and undoped ZBLAN

Manuscript received October 1, 1992; revised November 12, 1992. This work was supported by the Defense Advanced Research Projects Agency (L. N. Durvasula) and the Air Force Office of Scientific Research (H. Schlossberg).

The authors are with the Everitt Laboratory, University of Illinois, Urbana, IL 61801.

IEEE Log Numer 9206431.

cladding are 11 and 125 μm, respectively, and the numerical aperture for this multimode fiber is 0.15. Each end of the fiber was mounted in a ferrule and polished with standard Al_2O_3 grit techniques. Once polishing was completed, the fiber ends were butted directly against the cavity mirrors. The pump beam was provided by a CW ring dye laser ($\Delta\nu \sim 20$ GHz) driven by a 5 W Ar^+ laser and arrangements were made to scan the dye laser over the 640-660 nm region ($^5F_5 \leftarrow {}^5I_8$ transition) with a computer. A 10× microscope objective launched the pump (with an efficiency measured to be ~45%) into one end of the fiber through a flat dichroic mirror having a transmission at 650 nm of 85% and a reflectivity at 550 nm > 99.9%. The optical cavity consisted of the dichroic mirror and an output coupler with a transmission of 1, 3, or 5% at 550 nm. Both the 1 and 3% output coupling mirrors are flat whereas the 5% transmitting mirror has a radius of curvature of 15 cm. A second 10× objective collimated the beam emerging from the optical cavity and unabsorbed pump radiation was removed by a bandpass filter (transmission of 50% at 550 nm). The substrates of all of the cavity mirrors, except the 5% output coupler, are 3 mm thick, thus permitting 10× objectives to be used. The 6 mm thick, 5% output coupler required that the output collimator in this case be a 4× microscope objective.

Spectra were recorded by a photomultiplier or diode array coupled to a 1/4 m spectrograph having a reciprocal dispersion in first order of 3.2 nm/mm. The overall resolution of the system with 50 μm slits was, therefore, ~0.2 nm in first order. Energy measurements were made with a pyroelectric detector or a calorimeter and all experiments were carried out at room temperature.

Laser and fluorescence spectra for a 22 cm long fiber are shown in Fig. 1. Although other emissions are observed in the spectral region from 350 to beyond 800 nm, the dominant fluorescence arises from the green $^5S_2 \rightarrow {}^5I_8$ band. Spontaneous emission peaks at ~550 nm and falls off slowly towards the blue, giving the spectrum a full width (FWHM) > 13 nm. For longer fibers, peak emission shifts progressively to longer wavelengths as ground state absorption becomes more significant. When the broadband optical cavity is installed around the fiber, lasing occurs at several wavelengths in the 547.6–550.1 nm region and, as indicated by the inset to Fig. 1, the spectrum is dependent upon the pump wavelength (λ_p). This is a characteristic associated with the occupation of various sites in the glass host by Ho^{3+} ions and, consequently, inhomogeneous broadening of the gain profile [9], [10].

The variation of the output power at 549 nm with the 647 nm pump power is illustrated in Fig. 2 for the three values of output mirror transmission. For each output coupler, the threshold pumping power is 128 ± 5 mW (1.8 times larger than that observed for single mode fiber) [3] and the output power shows no signs of saturating with respect to either output coupling or the available pump power. Scattering in the fiber appears to be the dominant mechanism for the loss of power from the cavity. Despite

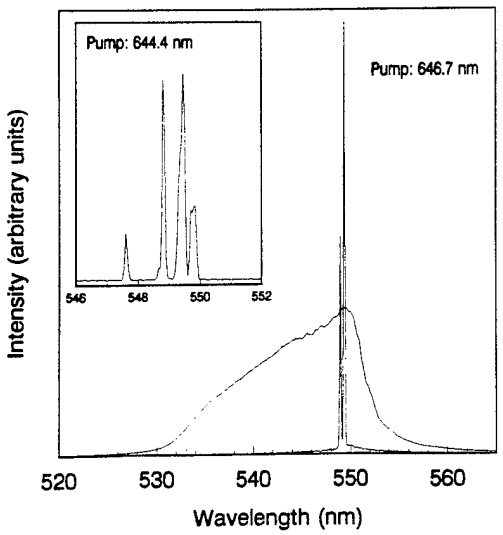

Fig. 1. Laser and spontaneous emission spectra for a 22 cm long Ho:ZBLAN fiber pumped at 646.7 nm with a CW ring dye laser. The intensity of the laser spectrum has, of course, been attenuated severely for illustrative purposes. The cavity output coupling was 1% and the inset shows the more complex spectrum observed wen the fiber is pumped at 644.4 nm. For all spectra, the pump power was ~250 mW.

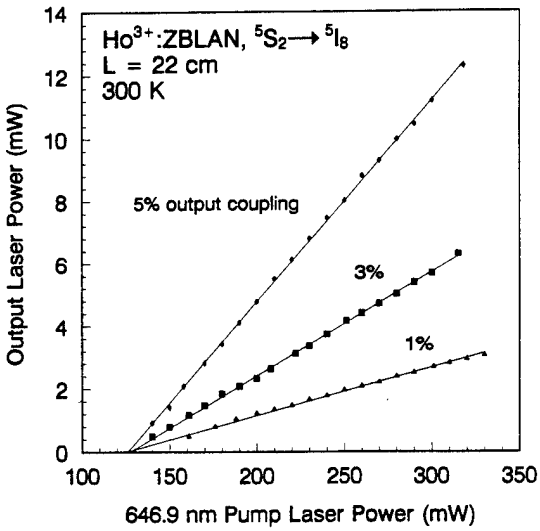

Fig. 2. Dependence of the 549 nm output power on pump power and mirror transmission. The pump wavelength was fixed at 646.9 nm and all data were acquired for a fiber length of 22 cm. The overall (for P = 318 mW) and slope efficiencies for the 5% output coupling data are 3.9 and 6.5%, respectively. The latter is 14.4% if the measured efficiency for injecting pump power into the fiber is accounted for. The 5% output coupler was fabricated on a 6 mm thick substrate which required the use of a 4× (rather than 10×) output collimating microscope objective. The solid lines represent the linear least squares fit to the data.

the large core diameter for this fiber, the maximum output power obtained from the laser for a 22 cm long fiber is 12.4 mW for 318 mW of pump power which yields an overall efficiency of 3.9%. The linear least-squares fit to the 5% transmission data corresponds to a slope efficiency (normalized to the launched pump power) exceeding 14%. Neither efficiency value has been corrected for the transmission of the dichroic mirror at 647 nm (85%).

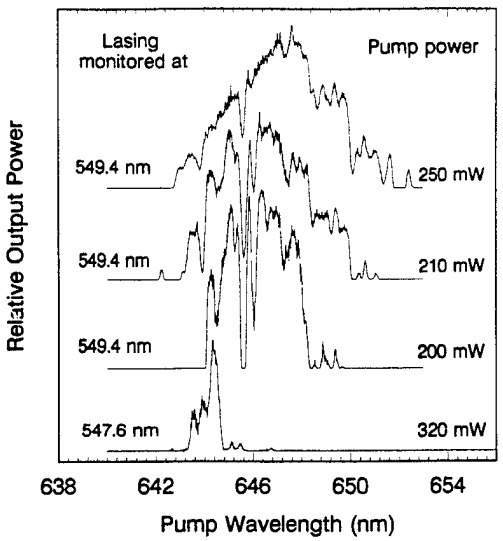

Fig. 3. Laser excitation spectra obtained by monitoring the output power of the Ho:ZBLAN fiber laser at 549.4 or 547.6 nm as the pump wavelength was scanned. In studying the 549 nm transition, the dye laser pump power (P) was fixed at various values between 200 and 320 mW (P = 200, 210, and 250 mW are illustrated) whereas the excitation spectrum shown for the 547.6 nm line was acquired for P = 320 mW.

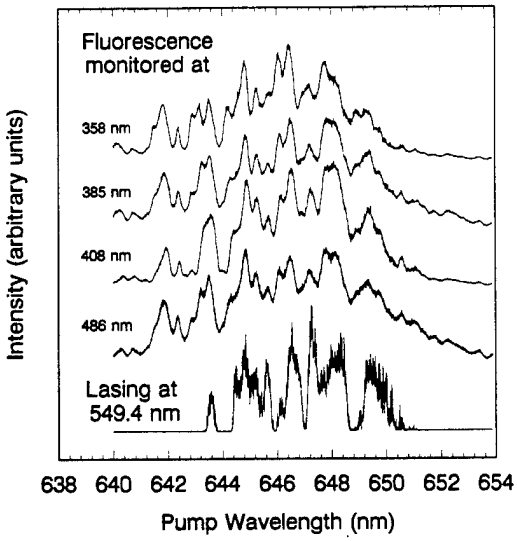

Fig. 4. Fluorescence excitation spectra acquired by recording the relative Ho^{3+} spontaneous emission intensity at the indicated wavelengths as the dye laser wavelength was scanned. Again, P was held constant at 250 mW. For comparison, a laser excitation spectrum for the 549 nm transition is also shown.

Also, the data of Fig. 2 were consistently reproducible to $\pm 5\%$. Under normal operation of this laser, mode beating and relaxation effects result in the output consisting of bursts of pulses occurring at a repetition frequency of ~ 100 Hz. Individual pulses within the bursts have temporal widths of ~ 800 ns (FWHM) and recur at a rate of ~ 100 kHz.

Fig. 3 shows the laser excitation spectra that were obtained by monitoring the output power at 549.4 or 547.6 nm as the pump wavelength was varied between 640 and 653 nm with the pump power (P) held constant. Spectra similar to these were measured for a number of the other $^5S_2 \rightarrow {}^5I_8$ lasing transitions but Fig. 3 illustrates the salient features of all of the spectra observed in these experiments. As P is increased from 200 to 250 mW (factors of ~ 1.6–2 larger than the threshold value), the excitation spectrum for the 549.4 nm transition broadens rapidly and for P = 250 mW has a width of ~ 5.3 nm FWHM. For this particular transition—the strongest of those observed—the range in pumping wavelength over which power can be extracted in the green is remarkable. As indicated by the lowest trace in Fig. 3, however, the excitation spectra for other laser lines are quite distinct. Even at the highest pump powers examined (330 mW), the spectrum for the 547.6 nm line, for example, is comparatively narrow. Qualitatively, the same behavior is observed for the other lines lying on the short wavelength side of the laser spectrum. Taken together, the increasing breadth of the laser excitation spectrum with higher pump power and the contrast between excitation spectra for different laser lines underscore the inhomogeneous broadening of the transition profiles as well as the site specific excitation of the rare earth ion in a glass host [2], [3], [10].

A prominent feature of the excitation spectra is their reproducible structure which contrasts with the fluorescence continuum of Fig. 1. To explore the origin of this structure and to determine the possible influence of excited state absorption (ESA) on the profiles of Fig. 3, *fluorescence* excitation spectra for several Ho^{3+} emission lines were measured while the green laser was in operation. That is, the relative intensity of the spontaneous emission from several Ho^{3+} excited states was recorded while the pump laser was again scanned in wavelength. Fig. 4 shows the results for the $^3D_3 \rightarrow {}^5I_7$ (358 nm), $^5G_4 \rightarrow {}^5I_8$ (385 nm), $^5G_5 \rightarrow {}^5I_8$ (408 nm) and $^5F_3 \rightarrow {}^5I_8$ (486 nm) transitions. These particular upper states were chosen for study because: 1) the state in question can be populated directly from the upper laser level ($^5S_2$) or the $^5I_{6,7}$ states by ESA (cf. dashed lines in Fig. 5), *or* 2) their lifetimes are among the largest of the states lying above the $^5S_2$ upper laser level [11, 12]. The latter is a reflection of energy gap considerations—Tanimura and coworkers [11] and Reisfeld *et al.* [12] demonstrated that the lifetimes of several Ho^{3+} states in fluorozirconate glass adhere to the (phenomenological) energy gap law. As discussed in [12], the minimum energy gap necessary for fluorescence from an ion excited state to dominate multiphonon relaxation is ~ 2200 cm^{-1} for ZBLAN glass.

Aside from minor differences, all of the fluorescence excitation spectra of Fig. 4 are not only identical but exhibit the same structure as the laser excitation spectrum for the 549 nm transition (bottom, Fig. 4). It is reasonable to conclude, then, that ESA has negligible impact on the excitation spectral profiles. Furthermore, preliminary spectra acquired for ~ 90 cm long fibers and P = 370 mW also display distinct features which indicate that the structure of Fig. 3 is not attributable to a changing distri-

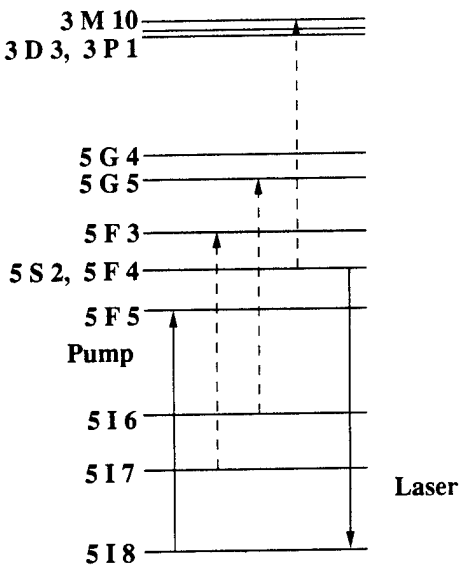

Fig. 5. Partial energy level diagram for Ho^{3+} indicating the pumped and lasing transitions (solid lines) as well as the states that are directly accessible by ESA of a pump photon (dashed lines).

bution of propagating modes (mode coupling) as the pump wavelength is varied. Consequently, it appears that the relative output power of this laser is determined by the $^5F_5 \leftarrow {}^5I_8$ absorption spectrum, and we tentatively attribute the bulk of the observed structure of Figs. 3 and 4 to transitions between specific Stark levels in the $^5S_2$ and $^5I_8$ manifolds. Corroborating evidence for this conclusion stems from the site selective spectroscopy of rare earth ions in fluorozirconate glasses that was performed by Adam *et al.* [13] in which Eu^{3+} served as a probe ion. Their results indicated that the rare earth ion occupies two types of lanthanum *substitutional* sites. Consequently, rare earth ions in fluorozirconate glass display higher symmetry than when doped into oxide glasses where the impurity ion resides at interstitial sites.

In summary, laser and fluorescence excitation spectra of the Ho:ZBLAN green fiber laser display considerable structure that is attributed to Stark sublevels of the $^5F_5$ and $^5I_8$ manifolds. Several prominent features in these spectra are consistent with Ho^{3+} occupying lanthanum substitutional sites in the glass. Output powers at 549 nm exceeding 12 mW have been obtained from a 22 cm long fiber for a slope efficiency of 14.4%.

ACKNOWLEDGMENT

The authors gratefully acknowledge the suggestions and assistance of S. G. Grubb, K. W. Bennett, R. S. Cannon, and W. F. Humer of Amoco.

REFERENCES

[1] J. Y. Allain, M. Monerie, and H. Poignant, "Blue upconversion fluorozirconate fibre laser," *Electron. Lett.*, vol. 26, pp. 166–168, 1990.

[2] J. Y. Allain, M. Monerie, and H. Poignant, "Room temperature CW tunable green upconversion holmium fibre laser," *Electron. Lett.*, vol. 26, pp. 261–263, 1990.

[3] J. Y. Allain, M. Monerie, and H. Poignant, "Characteristics and dynamics of a room temperature CW tunable green upconversion holmium fibre laser," in *Proc. 16th European Conf. Opt. Commun. (ECOC '90)*, vol. 1, pp. 575–578, Amsterdam, The Netherlands, Sept. 16–20, 1990.

[4] J. Y. Allain, M. Monerie, and H. Poignant, "Tunable CW lasing around 610, 635, 695, 715, 885 and 910 nm in praseodymium-doped fluorozirconate fibre," *Electron. Lett.*, vol. 27, pp. 189–191, 1991.

[5] R. G. Smart, J. N. Carter, A. C. Tropper, D. C. Hanna, S. T. Davey, S. F. Carter, and D. Szebesta, "CW room temperature operation of praseodymium-doped fluorozirconate glass fibre lasers in the blue-green, green and red spectral regions," *Opt. Comm.*, vol. 86, pp. 333–340, 1991.

[6] R. G. Smart, D. C. Hanna, A. C. Tropper, S. T. Davey, S. F. Carter, and D. Szebesta, "CW room temperature upconversion lasing at blue, green and red wavelengths in infrared-pumped Pr^{3+}-doped fluoride fibre," *Electron. Lett.*, vol. 27, pp. 1307–1309, 1991.

[7] A. C. Tropper, "Visible upconversion fiber lasers," Top. Conf. Compact Blue-Green Lasers (Opt. Soc. America, Santa Fe, NM, 1992), paper ThB1.

[8] J. Y. Allain, M. Monerie, and H. Poignant, "Tunable green upconversion erbium fibre," *Electron. Lett.*, vol. 28, pp. 111–113, 1992.

[9] K. Liu, M. Digonnet, K. Fesler, B. Y. Kim, and H. J. Shaw, "Broadband diode-pumped fibre laser," *Electron. Lett.*, vol. 24, pp. 838–840, 1988.

[10] F. Auzel, D. Meichenin, and H. Poignant, "Laser cross-section and quantum yield of Er^{3+} at 2.7 μm in a ZrF_4-based fluoride glass," *Electron. Lett.*, vol. 24, pp. 909–910, 1988.

[11] K. Tanimura, M. D. Shinn, W. A. Sibley, M. G. Drexhage, and R. N. Brown, "Optical transitions of Ho^{3+} ions in fluorozirconate glass," *Phys. Rev. B*, vol. 30, pp. 2429–2437, 1984.

[12] R. Reisfeld, M. Eyal, E. Greenberg and C. K. Jorgensen, "Luminescence of six J-levels of holmium (III) in barium zirconium fluoride glass at room temperature," *Chem. Phys. Lett.*, vol. 118, pp. 25–28, 1985.

[13] J. L. Adam, V. Ponçon, J. Lucas and G. Boulon, "Site selection spectroscopy in Eu^{3+}-doped fluorozirconate glass," *J. Non-Crystalline Sol.*, vol. 91, pp. 191–202, 1987.

Room-temperature fluorozirconate glass fiber laser in the violet (412 nm)

D. S. Funk, J. W. Carlson, and J. G. Eden

Everitt Laboratory, Department of Electrical and Computer Engineering, University of Illinois, Urbana, Illinois 61801

Received February 24, 1995

Continuous oscillation on the $^2P_{3/2} \rightarrow {}^4I_{11/2}$ transition of Nd^{3+} in a fluorozirconate glass (ZBLAN) fiber at room temperature has been observed. When pumped at ~590 nm, a Nd:ZBLAN fiber 39 cm in length lases in the violet at 412 nm and produces ~0.5 mW of power for 320 mW of pump power and a cavity output coupling of 0.4%. The breadth of the laser's excitation spectrum is ~12 nm (581–593 nm).

Upconversion fiber lasers offer an efficient approach to converting red or near-infrared photons into coherent visible or ultraviolet radiation. The fabrication and availability of rare-earth-doped fluorozirconate glass (ZBLAN) fiber has proven to be the key development in realizing visible fiber lasers because the characteristics of ZBLAN glass, combined with the inherent advantages of the fiber geometry, are responsible for the performance of these devices. Because of a phonon spectrum confined to low energies ($<3kT$, $T = 300$ K), the telluride or heavy-metal fluoride glasses such as ZBLAN minimize deactivation of rare-earth-excited states by multiphonon processes, thereby lengthening the effective lifetimes of ion excited states that are pivotal to the upconversion process.[1] In conjunction with the extended pump/gain medium interaction lengths afforded by fibers, this property of ZBLAN underlies the success in demonstrating a variety of cw, rare-earth-doped fiber lasers over the past five years.[2–6] The fiber geometry is particularly beneficial when the pump absorption is weak or the stimulated emission cross section is small, and, in numerous cases, transitions that have been demonstrated to lase at room temperature in ZBLAN fibers have required cooling for lasing to occur in a bulk fluoride crystal. Furthermore, the fiber length permits small rare-earth concentrations to be used in cases in which ion–ion interactions are detrimental to the overall efficiency of the system.

Wavelengths throughout the near-infrared and visible are now available from compact fiber lasers operating at room temperature, and recently what is to our knowledge the first ultraviolet fiber laser, based on Nd-doped ZBLAN fiber, was reported.[7] This Letter describes the demonstration of lasing on the $^2P_{3/2} \rightarrow {}^4I_{11/2}$ transition of Nd^{3+} at 412 nm in a ZBLAN fiber. At room temperature the device operates cw and ~0.5 mW of output power is obtained for ~0.4% output coupling. In 1989, Tong *et al.*[8] reported lasing at 413 nm from a Nd:$YLiF_4$ crystal cooled to below 40 K.

The active medium for these experiments is a Nd-doped ZBLAN fiber having a core diameter of 2.2 μm, a NA of 0.15, and a Nd concentration in the core of 1000 ppm (by weight). Consequently the cutoff wavelength is 400 nm. Two mirrors butted directly against the polished ends of the fiber formed the optical cavity. One of the mirrors is a dichroic through which the pump is launched into the fiber. It is flat and transmits ~0.3% at 412 nm and >95% at 590 nm. When a 10× microscope objective is used to couple the pump beam from an Ar-ion-pumped ring dye laser into the fiber, the launching efficiency is estimated to be 30%. The second mirror has a radius of curvature of 10 cm and a transmission of 0.1% at 412 nm. Therefore, the overall output coupling of the cavity is 0.4% and the power measurements reported here represent the sum of the outputs measured from both ends of the fiber.

A 5× microscope objective collimated the radiation emerging from the 0.1%-transmitting mirror, and spectra were recorded with a diode array coupled to a 0.25-m spectrograph having a reciprocal dispersion (in first order) of 6 nm/mm. Power measurements were made with a calibrated calorimeter, and the transient behavior of the laser was examined with a 500-MHz-bandwidth oscilloscope and a photomultiplier. All experiments were carried out at room temperature.

Figure 1 shows the spontaneous emission and laser spectra in the ~360–430-nm region for a Nd:ZBLAN fiber pumped at 590 nm. As reported previously,[7] two intense fluorescence peaks, centered at 381 and 412 nm, are observed and are attributed to $^4D_{3/2} \rightarrow {}^4I_{11/2}$ and $^2P_{3/2} \rightarrow {}^4I_{11/2}$ transitions of the Nd^{3+} ion, respectively.[8,9] Once the optical cavity is installed, lasing occurs at 412 nm and the measured spectral linewidth of the violet beam is <0.1 nm. As depicted in Fig. 2, the absorption of a 590-nm photon excites the $^4G_{5/2}$ state, which subsequently relaxes by multiphonon emission to populate the $^4F_{3/2}$ manifold. Upon absorbing a second pump photon, the ion is excited to states lying immediately above the $^4D_{3/2}$ level, which also relax nonradiatively to the $^4D_{3/2}$ and $^2P_{3/2}$ states. Joubert *et al.*[9] measured the spontaneous emission lifetimes for the $^4F_{3/2}$ "platform" state and the $^2P_{3/2}$ upper laser level to be 470 and 50 μs, respectively, in Nd:BaY_2F_8.

Measurements of the dependence of the 412-nm output power on the pump power (at 590 nm) are summarized in Fig. 3 for a fiber 39 cm in length. The onset of oscillation is observed when the pump power incident on the input optics is ~225 mW. Output powers approaching 0.5 mW have been recorded for a pump power of 320 mW. For pump powers beyond

0146-9592/95/131474-03$6.00/0

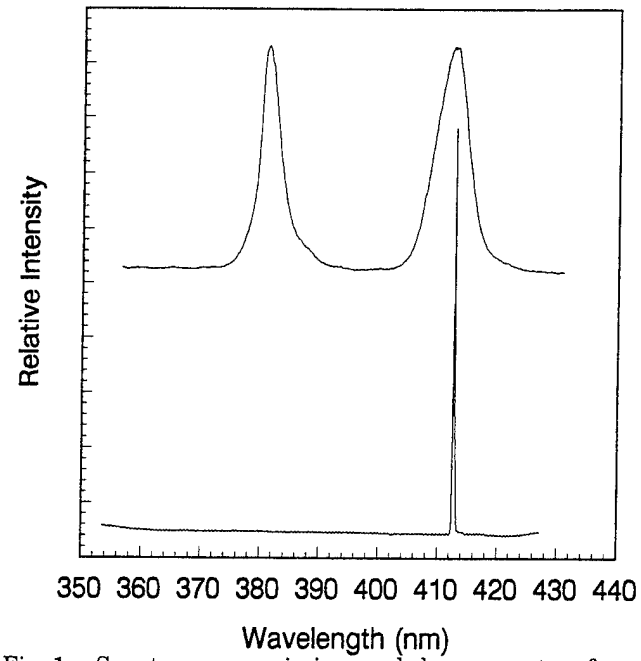

Fig. 1. Spontaneous emission and laser spectra for a Nd:ZBLAN fiber in the 360–430-nm spectral interval.

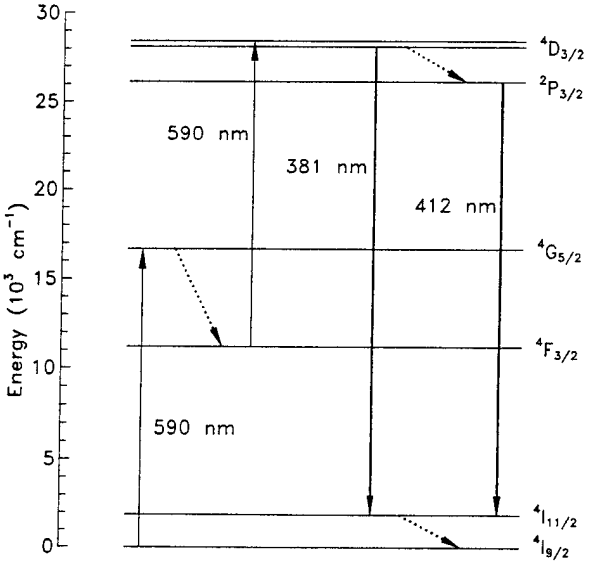

Fig. 2. Partial energy-level diagram of Nd^{3+} illustrating the absorption of two orange (~590 nm) photons followed by lasing on the $^4D_{3/2} \rightarrow {}^4I_{11/2}$ and $^2P_{3/2} \rightarrow {}^4I_{11/2}$ transitions of the ion in the ultraviolet and violet, respectively. The dotted lines represent nonradiative relaxation of an excited state by multiphonon emission.

~280 mW, the output shows signs of saturating, but, as indicated by the solid line in the figure, the overall slope efficiency exceeds 0.5%. Higher cavity output couplings have not yet been investigated, but it is expected that the optimal value will be >0.4% and that the output power and slope efficiency will both increase significantly over the values reported here. It should also be noted that the fiber exhibited several localized regions in which scattering was obvious. Continuing improvements in ZBLAN fiber fabrication will be necessary for the potential of this laser to be realized. Nevertheless, the performance of the Nd violet fiber laser compares favorably with that for the recently reported room-temperature Tm:ZBLAN fiber laser[10] that operates at 455 nm. Requiring two-color pumping (645 nm and 1.064 μm), the Tm:ZBLAN blue

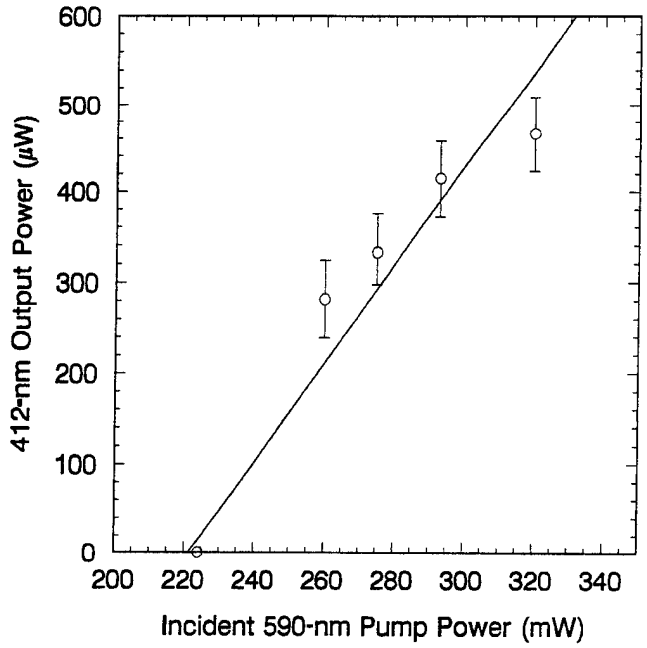

Fig. 3. Dependence of the violet laser output power on the 590-nm pump power incident on the input coupling optics. The estimated launching efficiency for the pump is 30%, and the cavity output coupling and fiber length are 0.4% and 39 cm, respectively. The solid line represents a slope efficiency of 0.5%.

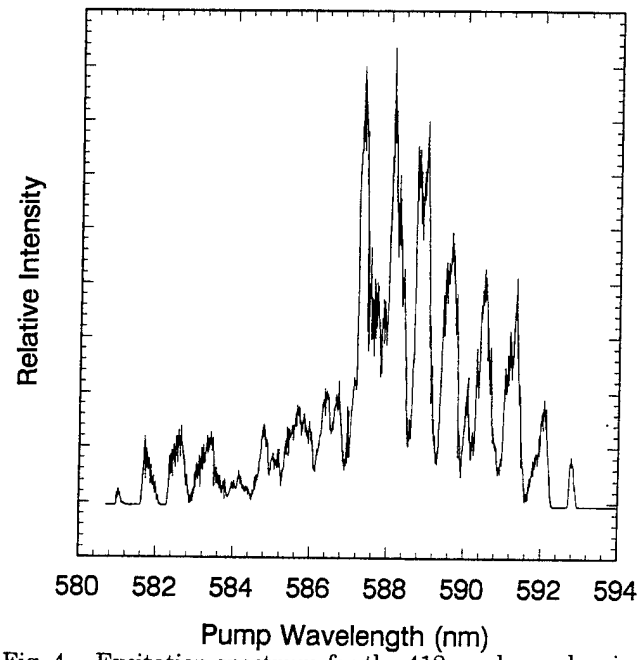

Fig. 4. Excitation spectrum for the 412-nm laser showing peak output power for pump wavelengths between ~587 and 589 nm. The periodic modulation of the spectrum is due to power reflected from the coupling optics.

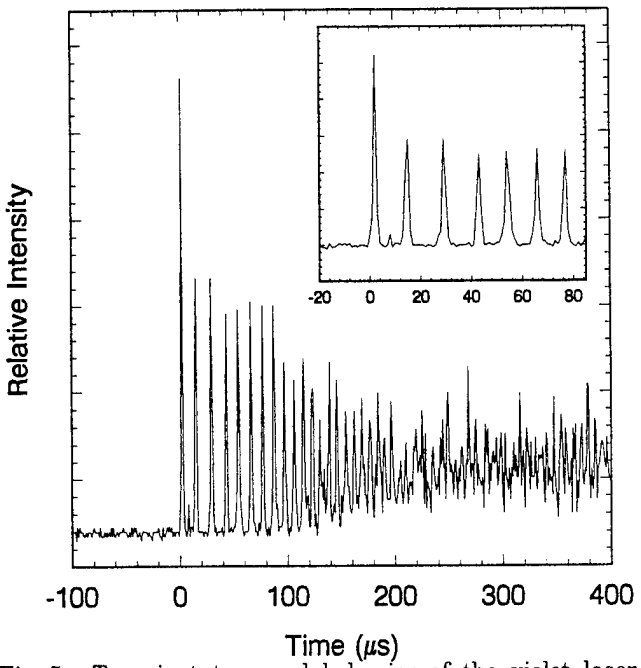

Fig. 5. Transient temporal behavior of the violet laser. The transition to cw operation occurs in ~250 μs. The inset is a magnified view of the first 80 μs of the waveform that was recorded for a pump power (incident on the fiber) of ~450 mW.

laser has a slope efficiency of 1.5% and a threshold pump power (red plus infrared) of ~420 mW.

Figure 4 displays the excitation spectrum that was obtained by recording the violet output power as the wavelength of the ring dye laser was scanned. Most of the structure in the spectrum results from interference effects between the input (flat) mirror and the fiber end that modulates the pump power coupled into the fiber by several percent.[7] Lasing is observed for pump wavelengths lying between 581 and 593 nm, but the device operates most efficiently when pumped in the 587–589-nm region. As observed previously for other rare-earth-doped ZBLAN fiber lasers, the Nd:ZBLAN laser is relatively insensitive to pump wavelength because the disordered nature of the glass host results in broadened gain and absorption spectral profiles.

A waveform representative of those observed when the pump beam (power incident on the fiber of ~450 mW) is chopped is shown in Fig. 5. Lasing begins ~0.5 ms after the pump is applied and, initially, exhibits relaxation oscillations having a periodicity of ~15 μs (the inset of Fig. 5 gives an expanded view of the early portion of the waveform). The amplitude of the pulses decreases rapidly, and, after ~250 μs, the output is continuous.

In summary, cw lasing in the violet (412 nm) has been observed from a Nd:ZBLAN fiber at room temperature. Roughly 0.5 mW of power has been obtained with an output coupling of 0.4%, and ~320 mW of pump power at ~590 nm. The excitation spectrum extends from 581 to 593 nm, and, although pumping this laser in the orange is not practical at present, preliminary experiments in which the fiber is excited at two wavelengths—680 and 805 nm—indicate that diode laser pumping of this oscillator should be feasible.

This research was supported by the U.S. Air Force Office of Scientific Research and the Advanced Research Projects Agency.

References

1. Strictly speaking, the visible fiber lasers utilizing ZBLAN glass as a host are generally not pumped by upconversion because the rare-earth concentrations are typically only 1000 ppm and the term upconversion has traditionally been reserved for interactions between two excited ions. However, the term has recently come to be associated with any process—such as the sequential absorption of two or more photons—by which low-energy (i.e., red or infrared) photons are converted to visible photons in a rare-earth-doped solid.
2. J. Y. Allain, M. Monerie, and H. Poignant, Electron. Lett. **26,** 166 (1990).
3. J. Y. Allain, M. Monerie, and H. Poignant, Electron. Lett. **26,** 261 (1990).
4. T. J. Whitley, C. A. Millar, R. Wyatt, M. C. Brierley, and D. Szebesta, Electron. Lett. **27,** 1785 (1991).
5. R. G. Smart, D. C. Hanna, A. C. Tropper, S. T. Davey, S. F. Carter, and D. Szebesta, Electron. Lett. **27,** 1307 (1991).
6. S. G. Grubb, K. W. Bennett, R. S. Cannon, and W. F. Humer, Electron. Lett. **28,** 1243 (1992).
7. D. S. Funk, J. W. Carlson, and J. G. Eden, Electron. Lett. **30,** 1859 (1994).
8. F. Tong, R. M. Macfarlane, and W. Lenth, in *Conference on Quantum Electronics and Laser Science,* Vol. 12 of 1989 OSA Technical Digest Series (Optical Society of America, Washington, D.C., 1989), paper THKK4.
9. M. F. Joubert, B. Jacquier, C. Linarès, and R. M. Macfarlane, J. Lumin. **47,** 269 (1991).
10. M. P. LeFlohic, J. Y. Allain, G. M. Stéphan, and G. Mazé, Opt. Lett. **19,** 1982 (1994).

Glass-Fiber Lasers in the Ultraviolet and Visible

David S. Funk and J. Gary Eden, *Fellow, IEEE*

Abstract— **The recent fabrication of rare earth-doped fluorozirconate (ZBLAN) glass fiber has spurred the development of a family of visible and ultraviolet fiber lasers pumped by upconversion. The performance of CW room temperature devices demonstrated to date is reviewed with emphasis on the recently reported Nd-doped ZBLAN fiber laser operating in the ultraviolet at 381 nm.**

I. Introduction

FEW COMPACT sources of CW coherent radiation are currently available in the spectral region below 450 nm. Applications in flow cytometry, reprographics, and stereolithography, for example, presently rely on gas lasers—primarily He–Cd (325 and 442 nm) and Ar^+ (333–364, 458–514 nm)—but solid-state sources have several potential advantages, including comparatively modest power consumption, reduced noise, and extended life. These considerations have prompted a pursuit of alternative sources, and much of the effort is being directed along three general lines: 1) Direct doubling of semiconductor lasers; 2) frequency-doubling of diode-pumped, rare earth-doped oxide crystalline lasers such as Nd:YAG and Nd:YVO_4; and 3) the development of short wavelength ($\lambda < 550$ nm) semiconductor diode lasers fabricated from II–VI and III–V materials, including ZnSe and GaN. Considerable strides have been taken in the last five years in advancing these technologies and although the relative advantages of each cannot be treated in detail here, several recent highlights should be noted. Commercial products based on the first two approaches listed above have been introduced—a direct-doubled AlGaAs laser system delivering 10 mW at 430 nm is now available, as is an intracavity-doubled, diode-pumped Nd:YAG microchip laser that offers up to 100 mW at 532 nm. Although diode lasers based on the ternary compound ZnS_xSe_{1-x} were demonstrated just four years ago [1], device lifetimes are steadily increasing but limited at present to ~1 hour. InGaN LED's, offering up to 3 mW of output power in the blue (450 nm) and a luminous intensity of 2 cd in the blue-green (500 nm) are now commercially available, but laser diodes have yet to be demonstrated [2].

A relatively new candidate is the upconversion laser which exploits the radiative lifetimes of excited states of trivalent rare earth ions (i.e., Er^{3+}, Tm^{3+}, ···) in fluoride crystals and glass fibers to efficiently convert red or infrared radiation into the visible or ultraviolet (UV). In addition to the features cited earlier that are characteristic of solid-state lasers in general, coherent sources pumped by upconversion have been demonstrated to be capable of multicolor operation, a distinct asset when considering applications in medical diagnostics and home entertainment.

This paper reviews the progress in developing CW room temperature lasers in rare earth-doped glass fibers that has been made over the past several years. First demonstrated in 1990, these systems now offer wavelengths ranging from the near ultraviolet into the infrared and two members of the family (Er:544 nm and Tm:480 nm) have been pumped efficiently by diode lasers. Of particular interest is the recently reported Nd-doped fluorozirconate glass-fiber laser that operates in both the ultraviolet (381 nm) and violet (412 nm). The first UV fiber laser to be pumped by any means, this oscillator is likely to be followed by other UV upconversion systems and provides access to applications for which photon energy ($\hbar\omega \geq 3$ eV) and physical size of the source are of primary importance.

II. Upconversion Fiber Lasers: General Characteristics

A. Brief History, Summary of Existing Systems

Upconversion is the term that has come to be associated with a variety of processes by which trivalent rare-earth ions in a crystal or glass absorb two or more infrared or red photons to populate high-lying excited electronic states (typically >20 000 cm^{-1} above ground). In heavily-doped crystals (>1 at.%), two (or more) adjacent ions can "pool" their energies in a cooperative process to produce one highly excited ion. However, since the rare earth doping level in fluoride glass fiber that is currently available is typically 1000 ppm, ion–ion interactions can usually be ignored and, as will be illustrated in the discussion to follow, the upper laser level is generally excited by the sequential absorption of at least two pump photons.

The first upconversion pumped laser was reported in 1971 by Johnson and Guggenheim [3], who obtained stimulated emission at 670 and 551 nm by flashlamp-pumping BaY_2F_8 crystals that were codoped with Er–Yb and Ho–Yb, respectively. It wasn't until 1987, however, that Silversmith et al. [4] at IBM demonstrated that CW lasing in the green (~550 nm) could be generated in Er-doped $YAlO_3$ crystals by a two color pumping scheme involving near-infrared photons. Since that time, upconversion-pumped lasers in several rare earth-doped crystals have been reported [5]–[10]. Output powers as large as 1.1 W (at 551 nm) have been produced [11], [12], and two systems operating at room temperature—Tm:BaY_2F_8 [13] and Er:$YLiF_4$ [14]—have recently been demonstrated.

Manuscript received April 27, 1995; revised June 26, 1995. This work was supported by the Air Force Office of Scientific Research and the Advanced Research Projects Agency.

The authors are with the Everitt Laboratory, Department of Electrical and Computer Engineering, University of Illinois, Urbana, IL 61801 USA.

IEEE Log Number 9414554.

TABLE I
SUMMARY OF RARE EARTH-DOPED FLUOROZIRCONATE GLASS-(ZBLAN)-FIBER LASERS PUMPED BY UPCONVERSION THAT HAVE BEEN DEMONSTRATED TO DATE. THE MAXIMUM SLOPE EFFICIENCIES OBTAINED FOR SPECIFIC LASING TRANSITIONS ARE ALSO INDICATED FOR SEVERAL SYSTEMS

Rare Earth(s)	Pump Wavelength(s) (nm)	Laser Wavelength(s) (nm)	T(K)	Slope Efficiency (%)	Reference(s)
Er	801	544, 546	300	$\leq$ 15	18, 22
	970	544, 546	300	25	19, 23-25
Ho	643-652	547.6-549.4	300	36	16, 26
Nd	582-596	381, 412	300	0.5 (412 nm)	20,21
Pr	476.5	610, 635, 695, 715, 885, 910	300	-	17
	1.01 μm and 835 nm	491, 520, 605, 635	300	12 (491 nm)	27-29
Pr/Yb	780-885	491, 520, 605, 635	300	3(@ 491 nm) to 52(@ 635 nm)	30
Tm	647.1, 676.4	455, 480	77	-	15
	1.064 μm and 645 nm	455	300	1.5	32
	1.112, 1.116, 1.1123 μm	480, 650	300	32 (480 nm)	31
	1.114-1.137 μm	480	300	13	34

Nevertheless, most upconversion lasers in rare earth-doped crystals suffer from several drawbacks: 1) operation at cryogenic temperatures (typically $\leq$90 K); 2) limited pump-gain medium interaction lengths owing to the size of available crystals and pump focusing considerations; and 3) narrow absorption linewidths associated with electronic transitions of rare earth ions in crystals, which complicates matching the wavelength of a diode pump laser to a specific rare earth absorption line.

The situation changed dramatically in 1990, when Allain, Monerie, and Poignant (CNET, France) reported that lasing had been obtained at a variety of visible wavelengths from Tm-, Ho-, or Pr-doped fluorozirconate glass fibers at room temperature [15]–[17]. In the intervening five years, stimulated emission has also been observed in Er:ZBLAN [18], [19] and Nd:ZBLAN [20], [21] fibers, and Table I summarizes the key characteristics of the lasers that have been demonstrated to date [22]–[33]. Emission wavelengths now available range from 381 nm in the near ultraviolet to beyond 2 μm [33] and output powers up to 300 mW in the red [27]–[30] and >100 mW in the blue (480 nm) [34] have been generated to date.

In addition to being compact, upconversion fiber lasers are noted for their efficiency and tunability. Slope and overall efficiencies (pump-to-output power) exceeding 30% and 28%, respectively, have been obtained [31] for the Tm:ZBLAN fiber laser at 480 nm, for example, and, as evidenced by Table I, slope efficiencies greater than 10% and pump power thresholds below 50 mW are commonplace among the upconversion fiber lasers. Several factors are responsible for the remarkable performance of these devices, including: 1) The pump/gain medium interaction lengths available with fiber hosts; 2) excitation intensities attainable with the confined pump beam; and 3) rare earth ion excited state lifetimes in fluoride glasses. The latter issue will be treated in detail in the next section, but a few comments concerning the beneficial

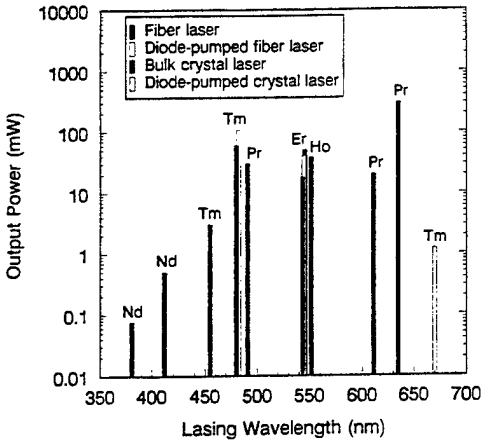

Fig. 1. Summary of the CW power currently available from room temperature, rare earth-doped glass-fiber and crystalline lasers. All of the laser transitions represented here are pumped by upconversion.

characteristics inherent with the fiber geometry itself are warranted. Fibers offer a convenient means for confining the pump beam as it interacts with the rare earth ion over lengths exceeding 1 m. This is an attractive property of fiber lasers since the lengths of bulk crystals are, in contrast, generally limited to a few centimeters. Consequently, the fiber geometry is particularly beneficial when the pump absorption is weak or the stimulated emission cross section for the rare earth transition of interest is small and, in the preponderance of cases, transitions which have been demonstrated to lase at room temperature in ZBLAN fibers have required cooling for lasing to occur in a crystal. Fiber hosts also allow for reduced rare earth concentrations to be used in those situations in which ion–ion interactions are detrimental to the pumping efficiency or increase the upper laser level deactivation rate. Furthermore, since the cross-sectional area of the core for a single-mode fiber in the visible is on the order of 10 μm^2, pump intensities beyond 10^6 W cm^{-2} are readily achievable, even for moderate power inputs (100 mW). The small core diameters for the fiber also account for the beam quality of upconversion fiber lasers, which typically produce radiation in the fundamental transverse (spatial) mode—LP_{01}.

Because the host is a disordered medium, rare earth-doped glass fibers exhibit absorption and emission profiles that are broad compared to those characteristic of a crystal. The breadth of the emission spectrum and its negative impact on the stimulated emission cross section are compensated for by the fiber length and the pumping intensities discussed earlier. Emission linewidths (FWHM) > 2 nm are typical of the rare-earth ions in fluorozirconate glass (cf., Fig. 2) and several of the upconversion fiber lasers have been tuned continuously more than 5 nm. The red (605, 635, 695 nm) and near-IR (715, 885, 910 nm) transitions of the Pr:ZBLAN fiber laser, for example, have each been tuned over a > 10-nm region [17], [27]. Similar results have been obtained for the green (λ ~550 nm) laser line of Ho:ZBLAN [16].

The broad absorption spectra associated with rare-earth ions in glasses have favorable implications for pumping upconversion fiber lasers with diode lasers. Fig. 3 shows the excitation

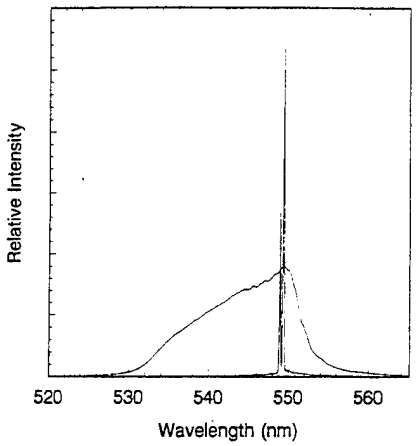

Fig. 2. Laser and spontaneous emission spectra for a ZBLAN fiber doped with 1000 ppm of Ho. The fiber was pumped in the red ($\lambda_p = 646.7$ nm) by a ring-dye laser. Note that the width of the fluorescence spectrum is >13 nm (FWHM) and that lasing on two transitions near the peak of the fluorescence profile ($\lambda \sim 549$ nm) is observed.

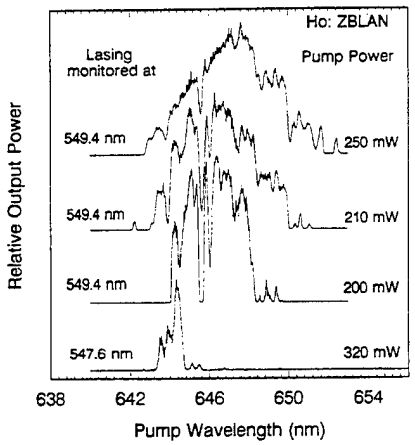

Fig. 3. Excitation spectra for the green ($\lambda \sim 550$ nm) Ho:ZBLAN fiber laser. Results are shown for four pump power levels and, as indicated, the spectra were obtained by monitoring power on one of two laser lines (549.4 or 547.6 nm).

spectrum for the green Ho:ZBLAN laser when pumped in the red ($\lambda \sim 646$ nm). Note that the profile is inhomogeneously broadened, which is a result of the occupation of various sites in the glass host by Ho^{3+} ions. As will be seen later for Nd:ZBLAN fibers, the breadth of the excitation spectrum of Fig. 3 (FWHM $\sim$ 4–5 nm) is representative of those for the other rare earth ions in fluorozirconate glass—a characteristic that considerably simplifies matching available diode laser wavelengths with a specific ion pumping transition. In the case of holmium, for example, III–V semiconductor-diode lasers (AlGaInP) generating more than 100 mW in the red ($\lambda \sim$ 645–650 nm) are now available and suitable for pumping this or other fluorozirconate fiber upconversion lasers. Diode-laser pumping of the Er:ZBLAN and Tm:ZBLAN fiber lasers at 544 and 480 nm, respectively, has already been achieved with gratifying results [22], [24], [25], [34]. In the case of the Er:ZBLAN system, 18 mW has been produced in the green with a slope efficiency of 25% and, for 150 mW of pump power at 971 nm and a cavity output coupling of 96%, an overall efficiency of ~10% has been achieved [24], [25]. By pumping Tm-doped fluorozirconate fiber with two tunable InGaAs diode lasers, Sanders *et al.* [34] obtained more than 100 mW of output power at 480 nm and 300 K.

B. *Excited State Lifetimes, Multiphonon Relaxation*

Since the realization of an upconversion laser hinges on the excitation of high-lying (>20 000 cm^{-1}) ion-excited states with comparatively low-energy photons ($\hbar\omega \approx$ 10 000–17 000 cm^{-1} or ~1.2–2.1 eV), the sequential absorption of two or more pump photons is required and it is critical that a minimal fraction of the energy invested in populating the upper laser level (or intermediate "storage" states) is dissipated by nonradiative mechanisms.

A partial energy level diagram of the Er^{3+} ion (after [24] and [25]) is shown in Fig. 4. As noted earlier, pumping of the $^4S_{3/2} \rightarrow {}^4I_{15/2}$ transition of Er^{3+} (544 nm) in ZBLAN fiber by an InGaAs diode laser (970 nm) was recently demonstrated [24], [25] and the two-step process believed to be responsible for populating the upper laser level is also illustrated in the figure. In this particular scheme, the lifetime of the intermediate state, $^4I_{11/2}$, is pivotal since efficiently populating the upper laser level requires that a second 970 nm photon be absorbed by the ion before the $^4I_{11/2}$ species is deactivated. The lifetime of this and other rare earth ion-excited states is strongly dependent upon the host and note from Fig. 4 that the Er^{3+} excited-state lifetimes in silica and fluorozirconate glass typically differ by several orders of magnitude. Interaction of the excited ion with the crystalline or glass host through multiphonon processes is responsible for this difference, and Fig. 5 illustrates the role of phonons in determining the lifetime of excited rare-earth ions [35]–[38]. The multiphonon emission rate (W) is shown as a function of the energy gap ΔE, which is defined as the energy defect between the ionic state in question and the next lower-lying excited state. Regardless of the host—glass or crystal—the excited-state decay rate arising from phonon emission obeys the phenomenological energy gap law that can be expressed as $W = C\exp(-\alpha\Delta E)$ where C and α are constants ($1.88 \cdot 10^{10}$ s^{-1} and $5.77 \cdot 10^{-3}$ cm, respectively, for fluorozirconate glass) [39], [40] and $\alpha = (a\hbar\omega)^{-1}$ where $\hbar\omega$ is the highest phonon energy in the host spectrum. Note from Fig. 5, that multiphonon emission is most severe for the borate and silicate glasses whose phonon spectra are known to extend in energy up to ~1000 cm^{-1}. For ZBLAN glass (which is composed of the fluorides of zirconium, barium, lanthanum, aluminum, and sodium) and other heavy metal-bearing hosts such as LaF_3, however, the phonon spectra are restricted to lower energies ($\hbar\omega < 600$ cm^{-1} for ZBLAN), and the multiphonon emission rate is dramatically reduced.

The values of ΔE associated with the upper laser levels for several upconversion fiber lasers are also given in Fig. 5, as are the inverse lifetimes of two rare earth ion excited states, $Nd^{3+}(^4D_{3/2})$ and Er^{3+} $(^4S_{3/2})$, in specific hosts. Lasing has been obtained for ion excited states having ΔE values ranging from ~2000 cm^{-1} to beyond 7000 cm^{-1}, but it is clear that

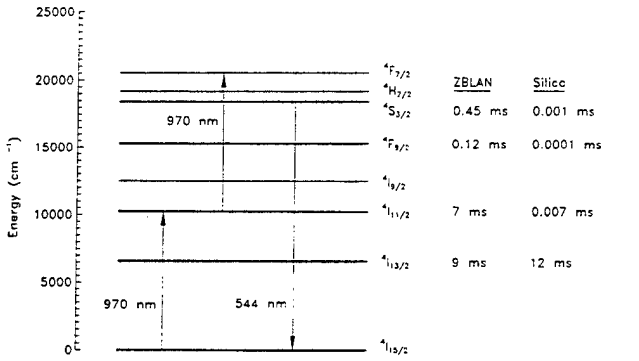

Fig. 4. Partial energy level diagram for Er^{3+} showing the lifetimes of several excited states for the ion when the host is silica or fluorozirconate glass (ZBLAN), after [24] and [25]. The excitation steps (for a pump wavelength of 970 nm) and the laser transition in the green are also indicated.

small values of ΔE ($\lesssim$3000 cm^{-1}) place increasing demands on the choice of host. Considering the $^4S_{3/2}$ state of Er^{3+}, for example, the multiphonon emission rate in ZBLAN glass is lower than the $^4S_{3/2}$ inverse lifetime and lasing on the $^4S_{3/2} \rightarrow {}^4I_{15/2}$ transition is readily observed at room temperature in fluorozirconate glass fibers, whereas nonradiative losses in oxide glasses (and crystals such as YVO_4) are prohibitive. The data of Fig. 5 underscore the importance of multiphonon processes and, therefore, the choice of host in determining the viability and performance of an upconversion laser. It is fair to say that the development of ZBLAN glass fiber is the primary factor responsible for the existence of this new family of lasers.

III. Nd:ZBLAN UV and Violet Fiber Laser

Recently, lasing on the $^4D_{3/2} \rightarrow {}^4I_{11/2}$ and $^2P_{3/2} \rightarrow {}^4I_{11/2}$ transitions of Nd^{3+} in ZBLAN fibers at 381 and 412 nm, respectively, has been demonstrated [20], [21]. A partial energy level diagram for Nd^{3+} is given in Fig. 6. The processes expected to be responsible for pumping the $^4D_{3/2}$ and $^2P_{3/2}$ excited states for the ion are also shown—the lasing transitions are represented by the heavy solid lines and dotted lines denote multiphonon relaxation. Upon absorbing a 590 nm photon ($\hbar\omega \sim 2.1$ eV), the ground-state species is excited to the $^4G_{5/2}$ level and subsequently decays by multiphonon emission to the $^4F_{3/2}$ state which has a spontaneous emission lifetime of 470 μs in BaY_2F_8 at 300 K [41]. The absorption of a second pump photon excites states lying immediately above the $^4D_{3/2}$ level at ~28 000 cm^{-1}. Phonon relaxation populates both the $^4D_{3/2}$ and $^2P_{3/2}$ states (separated by 2240 cm^{-1} in $YLiF_4$—[42]) and, although the ΔE values for the two states differ by only a few hundred cm^{-1}, the lifetime of the $^2P_{3/2}$ level against multiphonon emission in ZBLAN is roughly an order of magnitude larger than that for the $^4D_{3/2}$ state. For Nd in LaF_3, ΔE for the $^2P_{3/2}$ and $^4D_{3/2}$ states is 2300 and 1950 cm^{-1}, respectively [42]. At 300 K and 1 at.% Nd, τ_s, the inverse of the multiphonon emission rate, is 225 μs for the $^2P_{3/2}$ state and 13.5 μs for the $^4D_{3/2}$ level.

When a Nd:ZBLAN fiber, doped with 1000 ppm Nd, and having an NA of 0.15 and core and cladding diameters of 2.2 μm and 125 μm, respectively, is excited in the vicinity of 590 nm with a CW ring-dye laser, strong fluorescence peaks

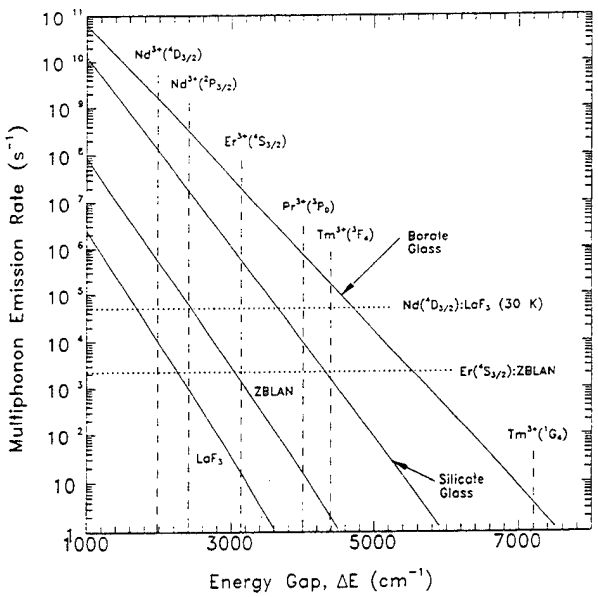

Fig. 5. Dependence of multiphonon emission (i.e., nonradiative relaxation) rates on the energy gap, ΔE, for various glass and crystalline hosts (adapted from [35] and [36]). Also indicated are: 1) The values of ΔE for the upper laser level of several upconversion fiber lasers (dashed vertical lines); and 2) the inverse lifetimes of the Er^{3+} ($^4S_{3/2}$) and Nd^{3+} ($^4D_{3/2}$) excited states in specific hosts (dotted horizontal lines). All of the data shown (with the exception of the $Nd^{3+}:LaF_3$ lifetime) are for $T = 300$ K.

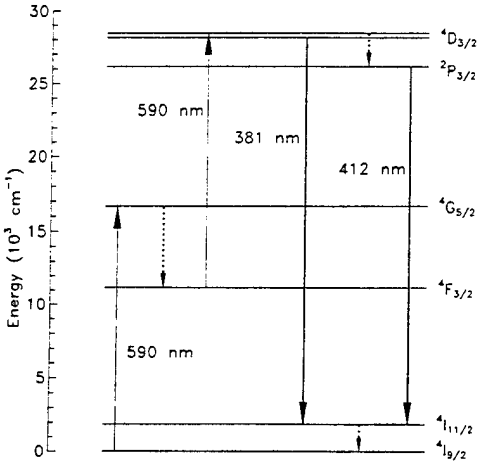

Fig. 6. Several of the excited states of Nd^{3+} illustrating the likely excitation pathway for the 381 and 412 nm lasers. The thick solid lines represent the lasing transitions, and the dotted lines denote multiphonon emission.

are observed extending from the mid-ultraviolet to almost 500 nm. As shown in Fig. 7, the 360–430 nm segment of the spectrum contains two intense emission lines at 381 and 412 nm whose profiles have spectral widths of ~4 and 6.5 nm, respectively. When an optical cavity is installed around the fiber, lasing occurs at the peak of each fluorescence profile. Spectral narrowing is clearly evident in Fig. 7, and the measured linewidth of the radiation is <0.1 nm for both transitions.

Experiments conducted at 381 nm involve an optical cavity consisting of two flat mirrors butt coupled to the fiber. Although both have reflectivities > 99.9% at 381 nm, one

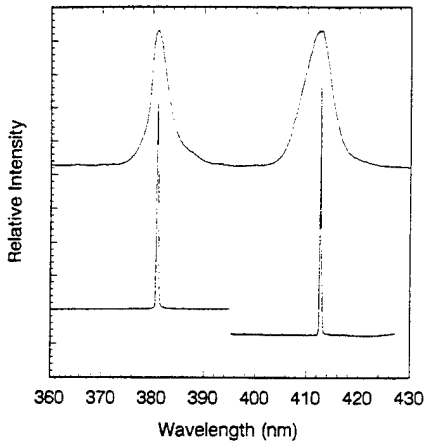

Fig. 7. Spontaneous and laser emission spectra in the 360–430 nm region for a Nd : ZBLAN fiber 45 cm in length and pumped at 590 nm. Lasing is observed at 381 and 412 nm (with two separate optical resonators—cf. Fig. 12).

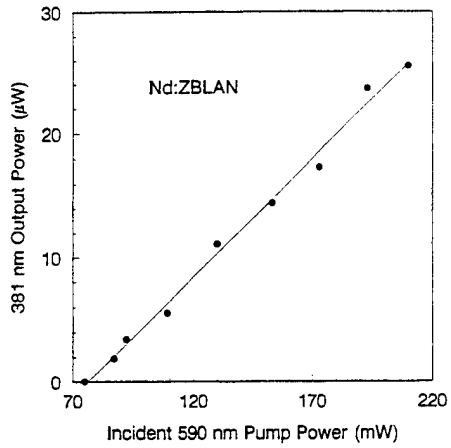

Fig. 8. Dependence of the UV laser (381 nm) output power on the 590 nm pump power incident on the input coupling optics. Since the estimated launching efficiency is 26%, the threshold pump power coupled into the fiber is ~20 mW. All of the data were recorded for a fiber 39 cm in length.

is a dichroic mirror having a transmission >95% at 590 nm, and it was through this mirror that the pump beam was launched into the fiber. Also, the output coupling mirror has a transmission >59% at 412 nm to intentionally suppress lasing on the $^2P_{3/2} \rightarrow {}^4I_{11/2}$ transition. The UV output beam is clearly visible with a fluorescent card, and Fig. 8 presents the results of measurements of the UV output power as a function of the 590 nm pump power. For a fiber 39 cm in length, the threshold pump power incident on the fiber is ~75 mW and the slope efficiency for pump powers up to ~210 mW is ~0.02%. Recalling that the transmission of the output mirror at 381 nm is <0.1%, it is expected that values of output coupling considerably higher than those studied to date will significantly improve the output power and slope efficiency of this laser. Also, since the estimated efficiency for launching the pump into the fiber is 26%, we note that the threshold power *coupled* into the fiber is ~20 mW. With the same cavity output coupling, but a longer fiber, the power output increases significantly, and the results for a 45-cm long fiber are illustrated in Fig. 9. Output powers as large as 74 μW for an incident pump power of 275 mW have been observed to date. The apparent saturation of the output power for pump powers beyond 220 mW likely results from defects in the fiber, rather than a fundamental limitation of the system itself. Since the number of scattering defects along the fiber increase with operating time, the deterioration of the fiber's optical quality appears to be associated with the UV intensities present in the core (tens of kW-cm^{-2}). It should be mentioned that this problem was not noticeable in our experiments with the green Ho : ZBLAN fiber laser [26].

Thrash and Johnson report single pulse lasing of Tm^{3+} at 347.9 nm at room temperature in BaY_2F_8 crystals codoped with Yb and Tm.

As shown in Fig. 10, the laser waveform exhibits spiking behavior. For illustrative purposes, the waveforms of Fig. 10 were recorded when the pump beam was chopped, but the same behavior was observed for continuous pumping. Threshold is reached ~1 μs following the start of the pump pulse and the output consists of ~10 ns pulses occurring at a repetition

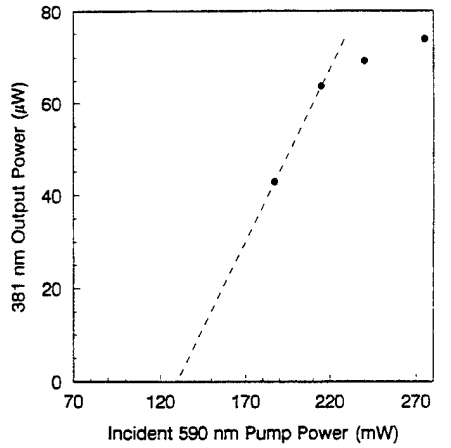

Fig. 9. Data similar to those of Fig. 8, except for a fiber 45 cm in length. An output power of 74 μW has been obtained for a cavity output coupling <0.1%, and higher output couplings have not yet been investigated.

frequency of 20–25 MHz. The time to reach threshold is a consequence of the stimulated emission cross section for the $^4D_{3/2} \rightarrow {}^4I_{11/2}$ transition at 300 K (<10^{-19} cm^2—[5]) and, as will be discussed later in connection with the violet laser, the periodicity of the relaxation oscillations is presumably a result of the multiphonon relaxation rate for the $^4D_{3/2}$ level.

As discussed earlier, an attractive aspect of upconversion lasers in glass fibers is the breadth of the spectral region over which the lasers can be pumped, and Fig. 11 shows the excitation spectrum obtained by scanning the pump wavelength while monitoring the relative output power. Note that operation of the laser is most efficient when it is pumped on the red side of the excitation spectrum ($\lambda_p > 592$ nm). All of the structure in the spectrum of Fig. 11 is reproducible, and the inset to the figure shows the wavelength dependence of the pump power reflected by the input coupling optics. The variation in pump power shown in the inset (several percent peak-to-peak) is responsible for the modulation of the excitation spectrum that is particularly noticeable for $582 \leq \lambda_p < 586$ nm.

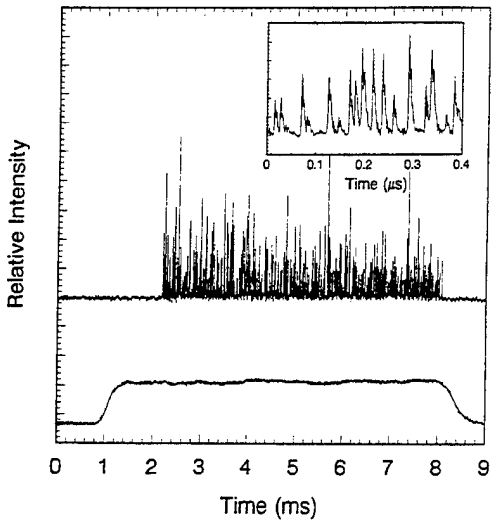

Fig. 10. Laser and pump waveforms for the UV Nd:ZBLAN fiber laser recorded for an incident pump power of 450 mW. The inset is an expanded view of a 400 ns portion of the laser waveform.

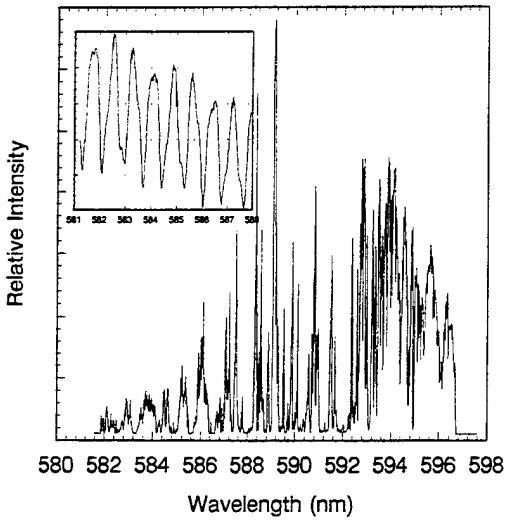

Fig. 11. Excitation spectrum for the 381 nm laser obtained for a pump power (incident on the input coupling optics) of ~450 mW.

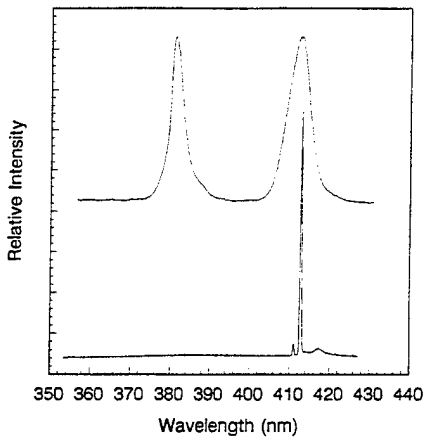

Fig. 12. Fluorescence and laser spectra for a 39-cm long Nd:ZBLAN fiber when the optical cavity is highly reflecting for $\lambda \sim 410$ nm. Strong oscillation is observed at 412 nm and, near threshold, a weaker line is recorded at 410.5 nm. The broad but faint feature peaking near 418 nm is due to spontaneous emission transmitted by the coating on the output mirror.

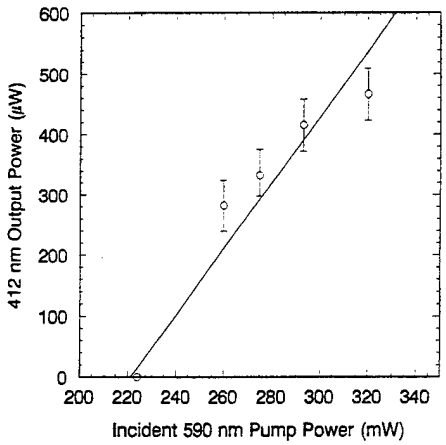

Fig. 13. Dependence of the violet laser (412 nm) output power on the 590 nm pump power incident on the input optics. The estimated launching efficiency is 30% and the total cavity output coupling is 0.4%. The solid line represents a slope efficiency of 0.5% and the length of the fiber is 39 cm.

Finally, although no attempts have yet been made to tune the 381-nm laser, the fluorescence spectrum of Fig. 7 and prior experience with upconversion fiber lasers suggest that the device should be continuously tunable over ~2 nm.

Similar experiments have been carried out for the $^2P_{3/2} \rightarrow {}^4I_{11/2}$ transition of Nd^{3+} and lasing has been observed at 412 nm in Nd:ZBLAN fibers typically 40 cm in length. For these studies, the optical cavity again consists of two mirrors butted directly against the polished ends of the fiber. One of the mirrors is a flat dichroic, transmitting ~0.3% at 412 nm, but >95% at 590 nm. With a 10× microscope objective, the efficiency for launching the pump beam into the fiber is estimated to be 30%. The second mirror has a radius of curvature of 10 cm and a transmission at 412 nm of 0.1%.

As shown in Fig. 12, lasing is observed at 412 nm, but when the device is operated just above threshold, oscillation also occurs on a weaker line at 410.5 nm. The linewidth of the 412 nm radiation was determined to be <0.1 nm—the same as that for the UV laser transition. Measurements of the variation of output power with the pump power (at 590 nm) are summarized in Fig. 13. The threshold pump power is ~225 mW, which corresponds to ~68 mW actually launched into the fiber. The solid line in the figure represents a slope efficiency of 0.5% and the maximum output power obtained to date for this optical cavity (coupling ≃0.4%) is ~0.5 mW. Fig. 14 shows the excitation spectrum that was recorded for the violet laser. Having a FWHM of ~5 nm, this spectrum is also modulated by the several percent of pump power that is reflected from the input coupling optics.

In contrast to the 381 nm laser, the violet transition exhibits true CW operation. Representative pump and laser waveforms for the 412 nm laser, illustrating the transient behavior of the laser, are given in Fig. 15. The onset of lasing is delayed by ~400 μs with respect to the leading edge of the pump pulse.

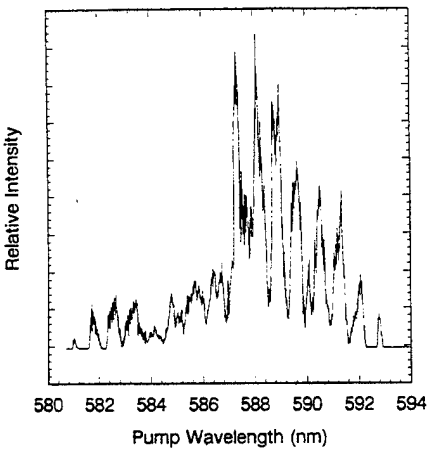

Fig. 14. Excitation spectrum for the violet Nd:ZBLAN laser (412 nm) showing peak output power for pump wavelengths in the 587–589 nm spectral region.

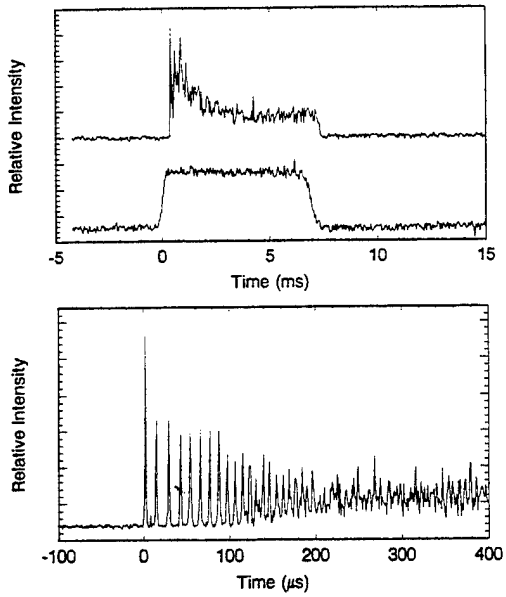

Fig. 15. Pump and laser waveforms typical of those observed for the 412 nm oscillator. The onset of lasing occurs > 300 μs following the start of the pump pulse and the transition to CW operation occurs in ~ 200 μs. An expanded view of the early portion of a laser waveform is shown in the lower box. These waveforms were acquired for a pump power of ~ 450 mW.

Initially, relaxation oscillations having a periodicity of ~ 15 μs are observed, but the amplitude of the pulses decays rapidly and, after ~ 200 μs, the device is operating CW although high-frequency noise is clearly present on the waveform.

The different temporal behavior of the violet and UV laser transitions is at least partially attributable to phonon relaxation. For the Nd^{3+} $^4D_{3/2}$ state (381 nm laser upper level), multiphonon losses prevent CW operation of the UV laser but permit it to emit in a stable relaxation oscillator mode. From Section II-B, however, recall that the phonon emission rate for the lower-lying $^2P_{3/2}$ level is roughly an order of magnitude lower than that for the $^4D_{3/2}$ state. It appears that this reduced nonradiative loss rate for the $^2P_{3/2}$ state is a critical factor in the violet laser's ability to operate continuously (following a brief period of decaying oscillations).

IV. Summary and Future Prospects for Upconversion Fiber Lasers

The fabrication of rare earth-doped fluorozirconate fiber has prompted the demonstration and development of a series of CW visible and ultraviolet lasers operating at room temperature. Offering wavelengths ranging from the near-UV (381 nm) through the near-IR and power levels beyond 100 mW in the red and blue and typically $>$ 1–10 mW elsewhere, these lasers are attractive for applications in low power applications in medical diagnostics, reprographics, and lithography which place a premium on beam quality, compactness, and modest power requirements.

In the next five years, it is likely that the power levels will surpass the 1 W milestone in the red, blue, and green. Two rare-earth:ZBLAN fiber lasers in the visible (Er and Tm) have already been diode-pumped, and others, including Pr and Ho, will undoubtedly be demonstrated in the near future. The commercial introduction of high-power semiconductor diodes at new wavelengths (notably, $\lambda < 670$ nm devices) and the exploitation of existing fiber lasers to pump a second fiber laser will rapidly expand the choice of lasers (wavelengths and power levels) available to the systems designer.

Now that the threshold of the ultraviolet ($\lambda = 400$ nm) has been crossed, it is inevitable that other, shorter wavelength UV lasers will follow [43].[1] In Nd:ZBLAN alone, several strong transitions lie to the "blue" of the 381 nm transition and the major concern is the transmission of ZBLAN glass in the UV. Of course, the development of fibers fabricated from other heavy metal glasses having lower energy phonon spectra or superior optical and mechanical properties would be of great value. We expect that the output power available from the Nd:ZBLAN violet laser will be improved from the current value of ~ 0.5 mW to beyond 5 mW by solely optimizing the cavity output coupling and fiber length. However, since pumping at 590 nm is, at present, impractical, new one or two color schemes for exciting both the 381 nm and 412 nm lasers in the deep red or near-infrared are under study.

[1]Thrash and Johnson report single pulse lasing of Tm^{3+} at 347.9 nm at room temperature in BaY_2F_8 crystals codoped with Yb and Tm.

References

[1] M. A. Haase, J. Qiu, J. M. DePuydt, and H. Cheng, "Blue-green laser diodes," *Appl. Phys. Lett.*, vol. 59, pp. 1272–1274, 1991.

[2] S. Nakamura, T. Mukai, and M. Senoh, "Candela-class high brightness InGaN/AlGaN double heterostructure blue light emitting diodes," *Appl. Phys. Lett.*, vol. 64, pp. 1687–1689, 1994.

[3] L. F. Johnson and H. J. Guggenheim, "Infrared-pumped visible laser," *Appl. Phys. Lett.*, vol. 19, pp. 44–47, 1971.

[4] A. J. Silversmith, W. Lenth, and R. M. Macfarlane, "Green infrared-pumped erbium upconversion laser," *Appl. Phys. Lett.*, vol. 51, pp. 1977–1979, 1987.

[5] R. M. Macfarlane, F. Tong, A. J. Silversmith, and W. Lenth, "Violet CW neodymium upconversion laser," *Appl. Phys. Lett.*, vol. 52, pp. 1300–1302, 1988.

[6] S. A. Pollack and D. B. Chang, "Ion pair upconversion pumped laser emission in Er^{3+} ions in YAG, YLF, SrF_2 and CaF_2 crystals," *J. Appl. Phys.*, vol. 64, pp. 2885–2893, 1988.

[7] D. C. Nguyen, G. E. Faulkner, and M. Dulick, "Blue-green (450 nm) upconversion Tm^{3+}:YLF laser," *Appl. Opt.*, vol. 28, pp. 3553–3555, 1989.

[8] T. Hebert, R. Wannemacher, W. Lenth, and R. M. Macfarlane, "Blue and green CW upconversion lasing in Er:$YLiF_4$," *Appl. Phys. Lett.*, vol. 57, pp. 1727–1729, 1990.

[9] M. E. Koch, A. W. Kueny, and W. E. Case, "A photon avalanche upconversion laser at 644 nm," *Appl. Phys. Lett.*, vol. 56, pp. 1083–1085, 1990.
[10] P. Xie and S. C. Rand, "Continuous wave, pair pumped laser," *Opt. Lett.*, vol. 15, pp. 848–850, 1990.
[11] R. A. McFarlane, "High power visible upconversion laser," *Opt. Lett.*, vol. 16, pp. 1397–1399, 1991.
[12] G. C. Valley and R. A. McFarlane, "1.1 W visible upconversion laser: Modeling and experiment," presented at the *OSA Top. Meet. Advanced Solid-State Lasers*, Sante Fe, NM, Feb. 1992.
[13] R. J. Thrash and L. F. Johnson, "Upconversion laser emission from Yb^{3+}-sensitized Tm^{3+} in BaY_2F_8," *J. Opt. Soc. Amer. B*, vol. 11, pp. 881–885, 1994.
[14] F. Heine, E. Heumann, T. Danger, T. Schweizer, G. Huber, and B. Chai, "Green upconversion continuous wave Er^{3+}:$LiYF_4$ laser at room temperature," *Appl. Phys. Lett.*, vol. 65, pp. 383–384, 1994.
[15] J. Y. Allain, M. Monerie, and H. Poignant, "Blue upconversion fluorozirconate fiber laser," *Electron. Lett.*, vol. 26, pp. 166–168, 1990.
[16] ——, "Room temperature CW tunable green upconversion holmium fibre laser," *Electron. Lett.*, vol. 26, pp. 261–263, 1990.
[17] ——, "Tunable CW lasing around 610, 635, 695, 715, 885 and 910 nm in praseodymium-doped fluorozirconate fibre," *Electron. Lett.*, vol. 27, pp. 189–191, 1991.
[18] T. J. Whitley, C. A. Millar, R. Wyatt, M. C. Brierley, and D. Szebesta, "Upconversion pumped green lasing in erbium-doped fluorozirconate fibre," *Electron. Lett.*, vol. 27, pp. 1785–1786, 1991.
[19] J. Y. Allain, M. Monerie, and H. Poignant, "Tunable green upconversion erbium fibre laser," *Electron. Lett.*, vol. 28, pp. 111–113, 1992.
[20] D. S. Funk, J. W. Carlson, and J. G. Eden, "Ultraviolet (381 nm), room temperature laser in neodymium-doped fluorozirconate fibre," *Electron. Lett.*, vol. 30, pp. 1859–1860, 1994.
[21] ——, "Room temperature fluorozirconate glass fiber laser in the violet (412 nm)," *Opt. Lett.*, to be published.
[22] J. F. Massicott, M. C. Brierley, R. Wyatt, S. T. Davey, and D. Szebesta, "Low threshold, diode-pumped operation of a green, Er^{3+} doped fluoride fiber laser," *Electron. Lett.*, vol. 29, pp. 2119–2120, 1993.
[23] D. Piehler, D. Craven, N. Kwong, and H. Zarem, "Laser diode pumped red and green upconversion fibre laser," *Electron. Lett.*, vol. 29, pp. 1857–1858, 1993.
[24] D. Piehler and D. Craven, "InGaAs laser pumped green upconversion fiber laser," presented at *Conf. Lasers and Electro-Opt., CLEO'94*, Anaheim, CA, 1994, paper CMK4.
[25] D. Piehler, D. Craven, and N. Kwong, "Green laser diode-pumped erbium fiber laser," presented at *Compact Blue/Green Lasers Conf.*, Salt Lake City, UT, paper CFA2, 1994.
[26] D. S. Funk, S. B. Stevens, and J. G. Eden, "Excitation spectra of the green Ho : fluorozirconate glass fiber laser," *IEEE Photon. Technol. Lett.*, vol. 5, pp. 154–157, 1993.
[27] R. G. Smart, D. C. Hanna, A. C. Tropper, S. T. Davey, S. F. Carter, and D. Szebesta, "CW room temperature upconversion lasing at blue, green and red wavelengths in infrared-pumped Pr^{3+}-doped fluoride fibre," *Electron. Lett.*, vol. 27, pp. 1307–1309, 1991.
[28] A. C. Tropper, J. N. Carter, R. D. T. Lauder, D. C. Hanna, S. T. Davey and D. Szebesta, "Analysis of blue and red laser performance of the infrared-pumped praseodymium-doped fluoride fiber laser," *J. Opt. Soc. Amer.*, vol. 11, pp. 886–893, 1994.
[29] Y. Zhao and S. Fleming, "High efficiency blue Pr^{3+}-doped fiber laser with high numerical aperture fiber," in *Adv. Solid-State Lasers Conf.*, Memphis, TN, paper PD 22-1, 1995 and *Opt. Commun.*, to be published.
[30] P. Xie and T. R. Gosnell, "Room temperature upconversion fiber laser in the red, orange, green and blue spectral regions," *Opt. Lett.*, vol. 20, pp. 1014–1016, 1995.
[31] S. G. Grubb, K. W. Bennett, R. S. Cannon, and W. F. Humer, "CW room temperature blue upconversion fibre laser," *Electron. Lett.*, vol. 28, pp. 1243–1244, 1992.
[32] M. P. LeFlohic, J. Y. Allain, G. M. Stéphan, and G. Mazé, "Room temperature continuous-wave upconversion laser at 455 nm in a Tm^{3+} fluorozirconate fiber," *Opt. Lett.*, vol. 19, pp. 1982–1984, 1994.
[33] J. Y. Allain, M. Monerie, and H. Poignant, "Tunable CW lasing around 0.82, 1.48, 1.88 and 2.35 μm in thulium-doped fluorozirconate fibre," *Electron. Lett.*, vol. 25, pp. 1660–1662, 1989.
[34] S. Sanders, R. G. Waarts, D. G. Mehuys, and D. F. Welch, "106 mW blue upconversion fiber laser pumped by laser diodes," in *Conf. Lasers and Electro-Opt., CLEO'95*, Baltimore, MD, 1995, postdeadline paper CPD23.
[35] W. J. Miniscalco, "Optical and electronic properties of rare earth ions in glasses," in *Rare Earth-Doped Fiber Lasers and Amplifiers*, M. J. F. Digonnet, Ed. New York: Marcel Dekker, 1993, pp. 19–133.
[36] H. H. Caspers, R. A. Buchanan, and H. R. Marlin, "Lattice vibrations of LaF_3," *J. Chem. Phys.*, vol. 41, pp. 94–99, 1964.
[37] S. A. Miller, H. E. Rast, and H. H. Caspers, "Lattice vibrations of $LiYF_4$," *J. Chem. Phys.*, vol. 52, pp. 4172–4175, 1970.
[38] A. A. Kaminskii, *Laser Crystals*, 2nd ed. Berlin: Springer-Verlag, 1990, pp. 328–329.
[39] K. Tanimura, M. D. Shinn, W. A. Sibley, M. G. Drexhage, and R. N. Brown, "Optical transitions of Ho^{3+} ions in fluorozirconate glass," *Phys. Rev. B*, vol. 30, pp. 2429–2437, 1984.
[40] R. Reisfeld, M. Eyal, E. Greenberg, and C. K. Jørgensen, "Luminescence of six J-levels of holmium (III) in barium zirconium fluoride glass at room temperature," *Chem. Phys. Lett.*, vol. 118, pp. 25–28, 1985.
[41] M. F. Joubert, B. Jacquier, C. Linarès, and R. M. Macfarlane, "A spectroscopic study of $BaY_2F_8:Nd^{3+}$," *J. Lumin.*, vol. 47, pp. 269–280, 1991.
[42] B. Jacquier, M. Malinowski, M. F. Joubert and R. M. Macfarlane, "Relaxation of the high lying excited states in Nd^{3+} doped $YLiF_4$, LaF_3 and YAG," *J. Lumin.*, vol. 45, pp. 357–359, 1990.
[43] R. J. Thrash and L. F. Johnson, "Ultraviolet upconversion laser emission from Yb^{3+} sensitized Tm^{3+} in BaY_2F_8," in *OSA Proc. Adv. Solid-State Lasers*, T. Y. Fan and B. H. T. Chai, Eds., vol. 20, pp. 400–402, 1994.

David S. Funk received the B.S. degree in physics at University of Puget Sound, Tacoma, WA, in 1989.

He is currently a graduate student in the Department of Physics at the University of Illinois, Urbana. His research interests include the study of rare earth-doped optical fiber and waveguide devices, and nonlinear optical waveguides.

J. Gary Eden (S'75-M'76-SM'82-F'88), received the B.S. degree in electrical engineering from the University of Maryland, College Park, in 1972, and the M.S. and Ph.D. degrees from the University of Illinois, in 1973 and 1976, respectively. He was awarded a National Research Council Postdoctoral Research Associateship from the Naval Research Laboratory, Washington, DC, in 1975.

Subsequently, he joined the staff of the Laser Physics Branch of the NRL, and during his tenure there made several contributions to the areas of visible and ultraviolet lasers and gas laser spectroscopy, including codiscovery of the KrCℓ laser (222 nm) and the demonstration of the optically pumped HgCℓ and XeF lasers. Since 1979, he has been a member of the faculty of the Department of Electrical and Computer Engineering at the University of Illinois, Urbana. He is also a member of the graduate faculty in physics and currently serves as Associate Dean of the Graduate College. His research group has demonstrated several new molecular lasers and amplifiers in the visible and near-IR (including CdI, ZnI and I_2 (500 nm) and developed laser spectroscopic techniques for studying the Rydberg and autoionizing states of diatomic and triatomic excimer molecules. He has also carried out extensive research on the growth of semiconductor and metal films by photochemical processes in the gas phase. His current research interests focus on upconversion lasers in waveguides and ultrafast, nonlinear techniques for generating coherent VUV radiation.

Dr. Eden is a Fellow of the American Physical Society and the Optical Society of America. He is currently serving as the Vice President for Technical Affairs of the IEEE Lasers and Electro-Optics Society (LEOS) and is the editor of the LEOS book series *Progress in Lasers and Electro-Optics*. He has published more than 130 papers, is the author of one book, and has been granted 12 patents.

Tuning, Temporal, and Spectral Characteristics of the Green ($\lambda \sim 549$ nm), Holmium-Doped Fluorozirconate Glass Fiber Laser

David S. Funk, S. B. Stevens, S. S. Wu, and J. Gary Eden, *Fellow, IEEE*

***Abstract*—The output power, tuning and temporal behavior of the green (539–550 nm), Ho-doped fluorozirconate glass (ZBLAN) fiber laser pumped in the red ($\lambda \sim 643$ nm) has been examined in detail. Fibers ranging in length from ~20–86 cm have been studied, and more than 38 mW of output power has been obtained from a 21 cm long fiber for 30% output coupling and 280 mW of absorbed pump power. By inserting two prisms into the optical cavity, the oscillator has been tuned over ~11 nm, and the emission spectrum of the free-running laser has been recorded as a function of pump power at both room temperature and 77 K. The self-pulsing (spiking) behavior of the laser and the influence of depletion of the Ho^{3+} ground state ($^5I_8$) population on the emission spectrum and efficiency of this system are discussed.**

I. Introduction

COMPACT sources of CW coherent radiation in the visible and ultraviolet (UV) are few in number and, until recently, virtually all of the commercially available systems were gas lasers. In the green and blue portion of the spectrum, the choices have been limited primarily to the He-Ne green transition (543.4 nm), Ar ion (458–514 nm), and He-Cd (442 nm). The dominance of gas lasers at these wavelengths for more than three decades is both remarkable and a testimony to the simplicity of gaseous systems, their excellent beam quality and the steady improvement of device performance (size reduction, new wavelengths, enhanced power, and lifetime) through engineering.

Although their longevity and adaptability continue to surpass expectations, gas lasers suffer from several well-known drawbacks including excessive power consumption and physical size and solid-state alternatives are being aggressively pursued. One promising class of UV, visible, and near-infrared lasers that has emerged over the past several years is the upconversion fiber laser. Based on rare earth-doped fluorozirconate glass (ZBLAN) fibers, this family of lasers was discovered in 1990 [1], [2] and offers power outputs in the red (635 nm) and blue (480 nm) exceeding 100 mW and overall efficiencies (pump-to-output) of ~10–15%.[1] Lasing in the UV and violet from Nd-doped ZBLAN fibers was recently reported [3], [4], and the available wavelengths now span the 380 nm to >2 μm region. The properties of these lasers have been described in more detail in [5].

The Ho:ZBLAN fiber laser operates in the infrared (1.2 and 2.0 μm), red (750 nm), and green ($\lambda \sim 549$ nm) and was the second of the visible upconversion fiber lasers to be demonstrated [2]. Although the green transition has been successfully pumped in the near-infrared (750 or 890 nm) [6], it is most efficient when pumped in the red (640–645 nm), and output powers >12 mW were reported in [2], [7], and [8]. Lasing on the green transition of Ho^{3+} had previously been obtained by Voron'ko *et al.* [9] and Johnson and Guggenheim [10] in Ho-doped CaF_2 and BaY_2F_8 bulk crystals, respectively, but in both cases, it was necessary to cool the crystals to 77 K. While it is perhaps not as well-studied as other upconversion fiber lasers, Ho:ZBLAN is known to be widely tunable and exhibits one of the highest slope efficiencies reported to date (36%, [7]). In this paper, the results of a series of experiments in which the temporal and spectral behavior of the Ho:ZBLAN fiber laser were characterized [11] are described.

II. Experimental Apparatus

The fibers for these experiments were fabricated from ZBLAN glass and have a Ho^{3+} concentration in the core of 1000 ppm molar and a NA of 0.15. Because the core and cladding diameters are 11 and 125 μm, respectively, the fiber is multimode at both the pump and laser wavelengths. Nineteen LP modes are propagating at 643 nm and more than 24 modes at 547 nm. Fiber lengths between 19.5 and 86 cm have been studied thus far, and virtually all of the experiments described here were carried out at room temperature.

Pumping of the fiber is provided by an Ar^+ laser-pumped, scanning ring dye laser having a linewidth (without etalons) of 20 GHz (~0.7 cm^{-1}) and operating in the red (630–690 nm). For all of the "free-running" (untuned) oscillator experiments,

Manuscript received August 30, 1995; revised December 1, 1995. This work was supported by the U. S. Air Force Office of Scientific Research (H. R. Schlossberg).

The authors are with the Everitt Laboratory, Department of Electrical and Computer Engineering, University of Illinois, Urbana, IL 61801 USA.

Publisher Item Identifier S 0018-9197(96)02558-4.

[1] In the literature, efficiencies of upconversion fiber lasers are specified in several ways. Since the efficiency with which pump power is launched into the fiber is dependent upon the NA and core diameter of the fiber as well as the input (coupling) optics, laser efficiency is often normalized to the launched power. By this definition, efficiencies have approached 40%. Also, *slope* efficiencies for several upconversion fiber lasers (such as Er (544 nm) and Tm (480 nm)) have exceeded 50% (cf. [5]). Most of the efficiencies reported here are referenced to the pump power absorbed by the fiber.

the optical cavity was formed by butt coupling the polished ends of the fiber against two flat mirrors. One was a dichroic mirror having maximum transmission (>95%) at 650 nm but a reflectivity >99.9% at 550 nm. It was through this mirror that the pump beam was launched into the fiber by means of a 10× microscope objective. The estimated launching efficiency for this arrangement is ~80%. One of five mirrors, having a transmission of 1.5, 3.1, 7.5, 11.6, or 31% at 550 nm, served as the output coupler for the optical cavity. Radiation emerging from the output coupler was collimated by a second 10× microscope objective and passed through a 550 nm bandpass filter ($\Delta\lambda$ = 50 nm FWHM). Power measurements were made with calibrated photoelectric or pyroelectric detectors and spectra were recorded by a diode array coupled to a 0.25 m spectrograph having a reciprocal dispersion (in first order) of 3.2 nm/mm. For 50 μm slits, the overall resolution of the detection system was ~0.2 nm in first order. Higher resolution scans of the laser spectrum were acquired with a 0.5 m Ebert spectrograph operating in second order. Laser waveforms were obtained with a Si photodiode and a digital signal analyzer having a bandwidth of 1 GHz.

Tuning of the oscillator was accomplished by installing two Brewster prisms and a concave mirror having a radius of curvature of 3 cm between the fiber and the output coupling mirror. The concave mirror served to collimate the radiation from the fiber, and the laser was tuned by rotating the output coupler.

III. Results and Discussion

A. Excited State Kinetics, Multiphonon Relaxation

Fig. 1 is a partial energy level diagram for Ho^{3+}, showing the states relevant to the 549 nm upconversion laser. The absorption of a pump photon by the ground state ion ($^5I_8$) populates Stark sublevels of the $^5F_5$ excited state which subsequently relax nonradiatively (by multiphonon processes) to the lower-lying $^5I_6$ and $^5I_7$ levels. It has previously been shown [12]–[15] that the excited states of Ho^{3+} in fluorozirconate glass adhere to the phenomenological energy gap law which expresses the nonradiative decay rate for a given state as

$$W = C\exp(-\Delta E/a\hbar\omega), \tag{1}$$

where ΔE is the energy separation between the excited Ho^{3+} state of interest and the next lowest-lying level, C and a are constants, and $\hbar\omega$ is the highest energy phonon in the host (ZBLAN) spectrum. For fluorozirconate glass, C and $a\hbar\omega$ have been determined to be $1.59 \cdot 10^{10}$ s^{-1} and 192.68 cm^{-1}, respectively [14]. In practical terms, the value of ΔE for each ion excited state determines if radiative decay will compete effectively with multiphonon emission. If ΔE for the state of interest exceeds a characteristic value for the host (and varies from host to host), then that state can be expected to be observed in emission. In fluorozirconate glass, for example, Reisfeld *et al.* [15] have noted that spontaneous emission has been observed from all Ho^{3+} excited states for which $\Delta E > 2100$ cm^{-1}. In the case of the $^5F_5$ manifold, ΔE is ~2200 cm^{-1} and the highest phonon energy ($\hbar\omega$) for

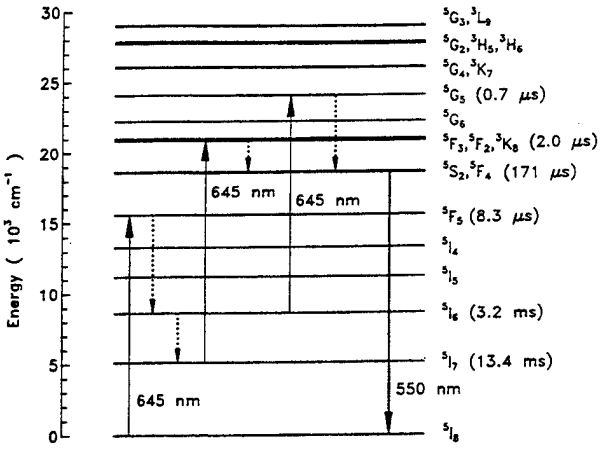

Fig. 1. Partial energy level diagram for Ho^{3+} showing the states and processes relevant to the $^5S_2 \rightarrow {}^5I_8$ green upconversion laser. The absorption of a pump photon is represented by a thin solid line and the laser transition by the bold line. Dotted lines denote multiphonon emission and the lifetimes of several excited states [7], [10], [12], [13] are also indicated.

ZBLAN glass is <600 cm^{-1} [12]–[15]. Consequently, the rate for deactivation of the $^5F_5$ state by multiphonon emission is $\sim 4 \cdot 10^5$ s^{-1} which gives rise to an overall $^5F_5$ lifetime of 8.3 μs. The lifetimes of both the $^5I_6$ and $^5I_7$ states, in contrast, are 3–13 *milliseconds*, making these levels well-suited as intermediate or "platform" states for the upconversion pumping process. The absorption of a second pump photon by the ion accesses (as indicated in Fig. 1) the $^5G_5$ or $^5F_3$ states which also relax nonradiatively to the comparatively long-lived $^5S_2$ level ($\tau \simeq 171$ μs). Lasing occurs on the $^5S_2 \rightarrow {}^5I_8$ transition of the ion which is calculated to have a stimulated emission cross-section at 300 K of $0.78 - 1.75 \cdot 10^{-20}$ cm^2 [15], [16]. Note that the overall quantum efficiency for this system is 2.25 eV/(2 · 1.92) eV ≃ 59%.

B. Ground State Depletion, Laser Spectra

Because the laser transition terminates on Stark sublevels of the ground state ($^5I_8$) of Ho^{3+}, depletion of the $^5I_8$ population has several significant implications for the performance of the green laser. One obvious area in which ground state depletion manifests itself is the absorption coefficient (α) at the pump wavelength, and Fig. 2 illustrates the results of measurements made at 643 nm for a fiber 21 cm in length. For ≳170 mW of launched pump power, the absorption coefficient has declined from its peak (zero field) value by more than 30% and, at P = 350 mW, $\alpha \simeq 3.3\%$ cm^{-1}. The role of ground state absorption in the data of Fig. 2 is perhaps more clearly illustrated in Fig. 3 in which the pump power transmitted by the 21 cm fiber is plotted as a function of the launched pump power. For ≲150 mW of launched power, the data display a quadratic dependence on pump power which is due to the combined effects of ground state *and* excited state ($^5I_6$, $^5I_7$) absorption. Above ≈180–200 mW of pump power, the $^5F_5 \leftarrow {}^5I_8$ absorption process appears to have saturated (owing to the large oscillator strength for the transition) [13] and excited state absorption accounts for the linear behavior of the data. These conclusions are similar to those reached by Allain, Monerie, and Poignant in [7].

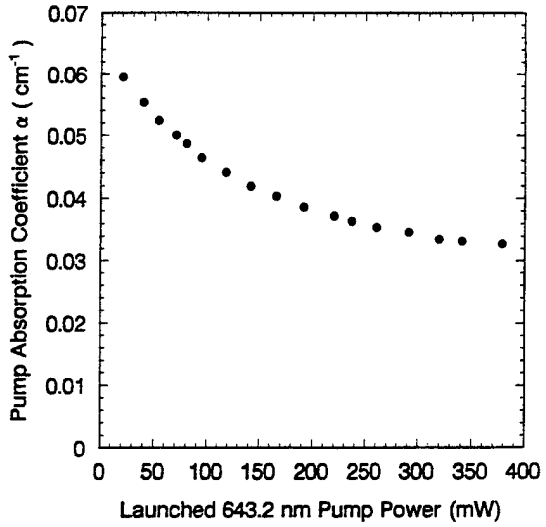

Fig. 2. Dependence of the absorption coefficient α on the pump power at 643 nm. These data were obtained for a fiber 21 cm in length.

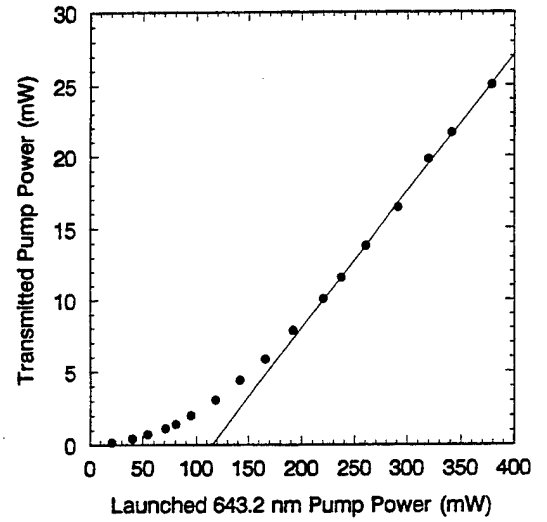

Fig. 3. Pump power at 643.2 nm transmitted by the 21 cm long fiber as a function of the launched power.

Extensive measurements of the $^5S_2 \rightarrow {}^5I_8$ laser spectra were made at 77 K and room temperature for several values of pumping power, and the results also reflect the influence of ground state absorption. A low resolution spectrum of the fluorescence and laser emission at 300 K is given in Fig. 4 for a fiber 21 cm in length. Because of reabsorption by the ground ($^5I_8$) state, the $^5S_2 \rightarrow {}^5I_8$ spontaneous emission spectrum emerging from the fiber shifts progressively toward the red as the fiber is lengthened. For this length of fiber, the breadth of the spontaneous emission profile is >13 nm (FWHM) and, when a high-Q cavity is installed, lasing occurs on two dominant transitions that coincide with peak fluorescence. Spontaneous emission spectra recorded from the sidelight (i.e., 90° to the fiber) and fluorescence emerging from one end of a 21 cm long fiber are both shown in Fig. 4, and the effect of ground state absorption is evident.

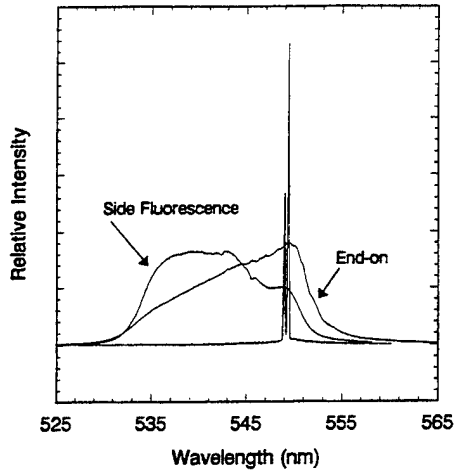

Fig. 4. Low resolution view of the fluorescence (both side and "end-on") and laser spectra for a ~21 cm long fiber pumped at 647.5 nm.

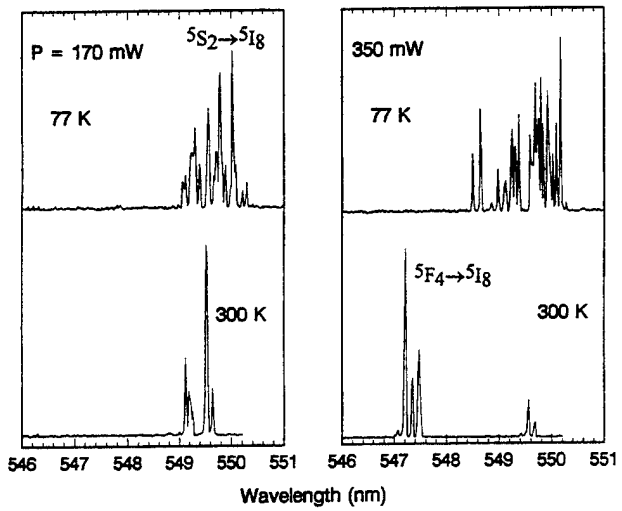

Fig. 5. Comparison of the laser spectra recorded for two values of pump power (incident on the pump optics) and operating temperature (77 and 300 K).

Some of the results recorded at various levels of pump power are summarized in Fig. 5 in which spectra produced by the untuned (free-running) laser when operating at 77 and 300 K and P = 170 and 350 mW are compared. All of the spectra were obtained from a fiber 19.5 cm in length. Although the spectra are congested and complex (partially due to the multiple sites occupied by the rare earth ion), several trends are clear. When the laser is operating at room temperature, increasing pump power results in the appearance and eventual dominance of lines at shorter wavelength. Specifically, at 300 K and P = 170 mW, the strongest laser lines are a pair lying between 549.1 and 549.6 nm. Increasing P beyond 250 mW leads to the appearance of several lines in the 547.2–547.6 nm interval and severe weakening of the longer wavelength transitions. The line at 547.2 nm is the most intense of those observed and, at still larger pump powers, this line remains dominant although new transitions at higher photon energies (547.05, 547.11 nm) are now present.

The emergence of the shorter wavelength features in the 300 K, 350 mW spectra is attributed to oscillation on the $^5F_4 \rightarrow {}^5I_8$ transition of Ho^{3+}. Because the $^5F_4$ and $^5S_2$ states lie in close proximity to one another (energy separation of 114 cm^{-1} in Ho:YAG) [17], the two have, understandably, been treated as essentially one state in previous studies of lasing in the green from Ho^{3+}. In Fig. 5, note that the new lines emerge ~74 cm^{-1} to the "blue" of the now-weakened features grouped around 549.6 nm. Since this gap is consistent with the expected $^5S_2 - {}^5F_4$ energy defect, the data suggest that: 1) the appearance of the short wavelength lines ($\lambda \sim 547$ nm) cannot be attributed to the $^5S_2$ state, 2) because the $^5F_4$ and $^5S_2$ populations are presumably in thermal equilibrium, intense pumping increases the $^5F_4$ population above a threshold value, thus resulting in stimulated emission on the $^5F_4 \rightarrow {}^5I_8$ transition, and 3) the stimulated emission cross-sections for the 547 nm ($^5F_4 \rightarrow {}^5I_8$) transitions are greater than those for the 549 nm ($^5S_2 \rightarrow {}^5I_8$) lines.

At 77 K, the behavior of the laser is markedly different, and the results point to the importance of the distribution of population among the Stark sublevels of the ground and $^5S_2$ states. All of the laser spectra acquired at this temperature consist of lines lying at $\lambda > 548.4$ nm but, as was the case for the room temperature data, the shortest wavelength lines (548.50, 548.65, 548.75 nm) are present only at the higher pump powers. These effects are attributed to partial depletion of several lower Stark sublevels of the ground state by the pump laser. For Ho^{3+} in LaF_3, for example, the $^5I_8$ state has 17 Stark sublevels ($Z_1 - Z_{17}$) and at 300 K the Boltzmann factor for the highest-lying of these (at 409 cm^{-1}) is 14%. For level Z_7, it has risen to ~50%. Consequently, the thermal populations of even the most energetic $^5I_8$ sublevels are significant at 300 K which has an obvious impact on the threshold pumping power for a specific line. From the 77 K, $P = 350$ mW data, however, it appears that pumping the ion at ~644 nm suppresses the populations of several lower-lying $^5I_8$ Stark sublevels to such a degree that a population inversion with respect to the $^5S_2$ state is produced. Also, the appearance of lines in the 77 K laser spectra lying to the *red* of the room temperature lines is likely the result of thermal relaxation of both the $^5S_2$ and $^5I_8$ state populations. Before leaving this section, two other points should be made. One is that the depletion of ground state sublevels by the pump was discussed previously in connection with excitation spectra for the green laser [8]. Specifically, the excitation spectrum for the shortest wavelength laser lines ($\lambda \sim 547$ nm) requires pumping wavelengths in a narrow region at the "blue" end of the $^5F_5 \leftarrow {}^5I_8$ absorption spectrum and pump powers in excess of 300 mW. Also, we note that the power produced by the Ho:ZBLAN laser is considerably higher at 77 K than at room temperature, but all of the data to be presented later were acquired at 300 K.

C. Tuning Characteristics

With the two prism configuration described earlier, a 40 cm long fiber has been tuned over a ~11 nm region, and the results of several experiments are summarized in Fig. 6 for an incident pump power (at 645 nm) of 430 mW. The top portion of the figure shows the superposition of a number of spectra recorded over the full tuning range of the fiber. Note that lasing was obtained from ~539–550 nm with a single fiber. In [7], tunability over the 539–553 nm spectral interval was also demonstrated with 2.7 μm core diameter fibers. Although three fibers having lengths of 45, 103, and 121 cm were necessary to span the entire region, tuning from 541 to 553 nm was observed with the 121 cm long fiber.

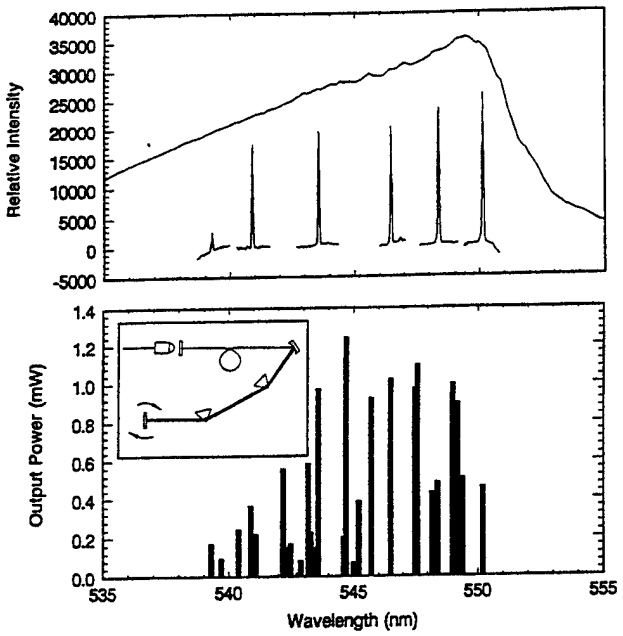

Fig. 6. Relative output power of the Ho:ZBLAN fiber laser at a variety of wavelengths in the green (~540–550 nm). Tuning was accomplished by installing two Brewster angle prisms inside the cavity, and all of the data were acquired with a ~40 cm long fiber and 430 mW of pump power at 645 nm. The upper half of the figure shows the spontaneous emission spectrum for the fiber and several laser spectra, representative of those observed as the laser was tuned. Only a few are shown for the sake of clarity. The lower portion of the figure illustrates the maximum output power that was obtained in the ~539–550 nm region for 1% of output coupling. The inset shows the experimental arrangement for the measurements. Although the threshold pump power for this arrangement was not measured precisely, it is estimated to be ~250 mW.

Attempts to tune the laser *continuously* over this 10 nm region were unsuccessful owing to the inhomogeneously-broadened gain profile and, perhaps, the core diameter of the fiber and polarization effects, but, at most wavelengths at which oscillation occurred, single line operation (linewidth < 0.1 nm) was obtained. The variation of the laser output power with wavelength is shown by the data in the lower portion of Fig. 6. Similar results for 20 and 80 cm fiber lasers are presented in Fig. 7.

D. Output Coupling Data

The dependence of laser output power on the absorbed pump power is illustrated in Fig. 8 for five values of cavity output coupling and a fiber 21 cm in length. Output couplings from 1–30% were studied in these experiments, and the largest output power obtained was 38 mW for 280 mW of absorbed pump power. Under these conditions, ~35% of the pump

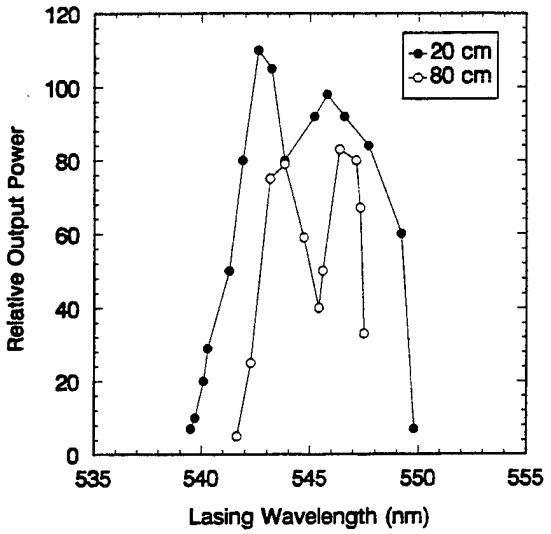

Fig. 7. Data similar to those of Fig. 6 illustrating the tuning characteristics of 20 and 80 cm fiber lasers.

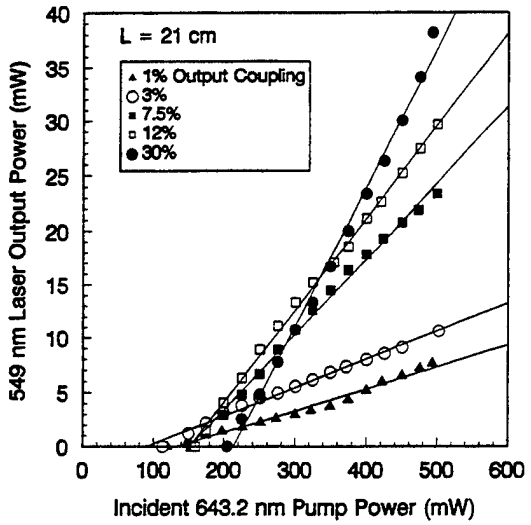

Fig. 8. Dependence of green output power on the incident pump power for a 21 cm long fiber and five values of cavity output coupling. Threshold pump powers (absorbed) varied between 66 and 130 mW, and the maximum slope efficiency and output power recorded were 24% and 38 mW, respectively. The solid lines represent linear, least-squares fits to the data.

power is not absorbed by the fiber. The threshold pump power ranged from 66–130 mW, and the maximum slope efficiency was 24%, which is to be compared to the value of 36% reported in [7] for a fiber ~45 cm in length and a core diameter of 2.7 μm. Note that the output power shows no signs of saturating with respect to the output coupling or pump power. The solid lines in the figure represent the linear least-squares fit to each set of data.

Since all of the pump power is not absorbed by this short fiber, the green output power depends on the reflectivity of the cavity output coupler in the red as well as its transmission in the green. This was verified by using a second mirror (99% reflecting at 650 nm) behind the output coupler to redirect the transmitted pump beam back into the fiber. The result was increased output power, particularly for those output couplers

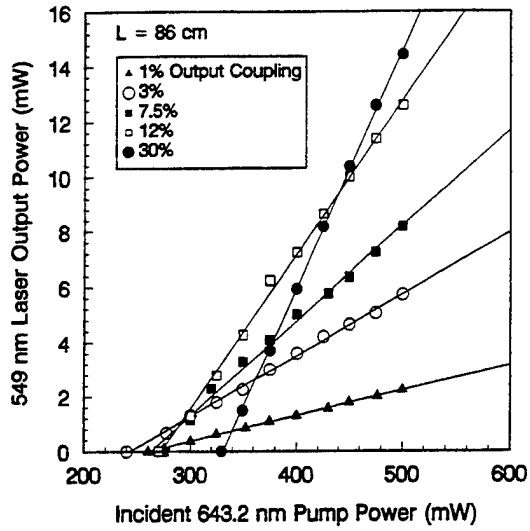

Fig. 9. Data similar to those of Fig. 8 for a fiber 86 cm in length. Threshold pumping powers (absorbed) ranging from 206–280 mW were measured (depending on the output coupling), and the largest output power obtained was 15 mW.

having low reflectivity at 650 nm. The data of Fig. 8 were obtained without the second mirror described above.

Similar data for an 86 cm long Ho:ZBLAN fiber are shown in Fig. 9. In this case, the maximum slope efficiency and output power recorded were 10% and 15 mW, respectively, and threshold pump powers ranged from 206 mW for 1% output coupling to 280 mW for 30% output coupling. Because of ground state absorption and the limited pump power available at present, the slope efficiency for the 86 cm fiber is considerably smaller than that for the shorter fiber. That is, absorptive losses from the weakly-pumped portion of the fiber limits the efficiency of the device and suggests that pumping from both ends of the fiber will be beneficial to overall performance. From the data of Figs. 8 and 9, one can readily extract the variation of the laser threshold pump power and slope efficiency with output coupling, and Fig. 10 illustrates the results. Although the threshold pump power increases linearly with output coupling (T), the slope efficiency appears to rise at a sublinear rate for $T > 10$–15%, but more measurements at still higher values of output coupling will be necessary before firm conclusions can be reached.

E. Temporal Behavior of the Laser

For the pumping wavelength and power range of these experiments, the Ho:ZBLAN fiber laser operates in a quasi-CW mode. Specifically, it exhibits self-pulsing behavior, and Fig. 11 shows waveforms typical of those observed when the untuned laser is operating in the steady state. The top trace is a 50 ms segment of the waveform which consists of bursts of pulses having a duration of ~5 ms and occurring at a repetition frequency of ~100 Hz. An expanded view of a laser waveform is given in the lower portion of Fig. 11. The individual pulses ("spikes") within the bursts have temporal widths of 1 μs FWHM and recur at a rate of ~100 kHz. By varying the alignment of the input microscope objective with respect to

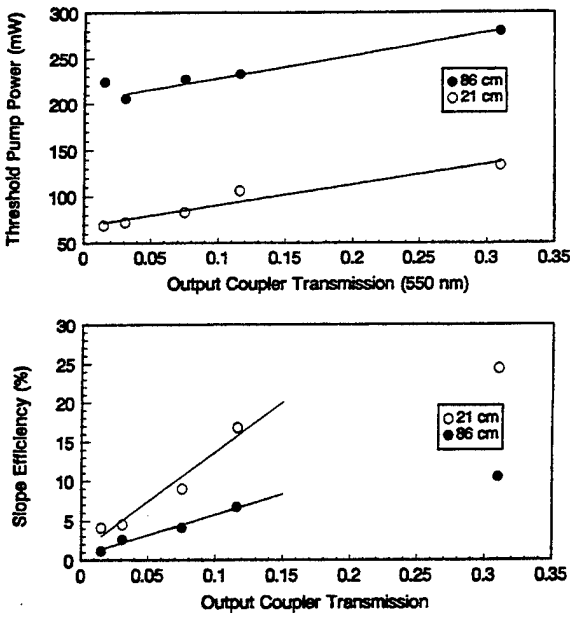

Fig. 10. Threshold pump power (top) and slope efficiency for the green Ho:ZBLAN laser as a function of the cavity output coupling (T). As denoted by the solid lines in the lower portion of the figure, the slope efficiency shows evidence of saturation for $T \gtrsim 15\%$.

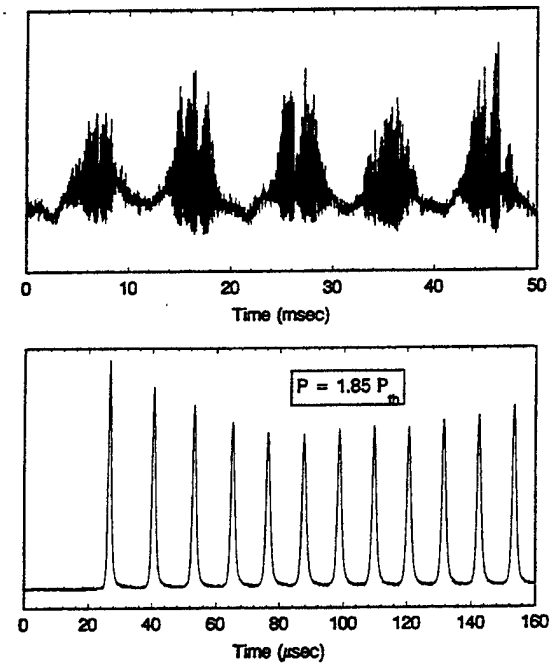

Fig. 11. Waveforms for the Ho:ZBLAN laser. (Top) 50 ms segment of the laser waveform for steady state conditions and a pumping power of 1.85× the threshold value ($P_{\rm th}$). (Bottom) Expanded view of a segment of a typical laser waveform. The individual pulses have temporal widths (FWHM) of 1–2 μs.

the fiber, it was possible to eliminate the bursts and obtain steady self-pulsing at the same frequency.

This behavior is similar to that reported for upconversion lasers in bulk crystals such as the Er^{3+} transition at 551 nm in fluoride crystals for which self-pulsing is now a familiar phenomenon [18]–[21]. Self-pulsing or "spiking" has previously been observed in erbium-doped infrared fiber lasers [22] and upconversion fiber lasers [1], [2] as well, and this phenomenon is common to solid-state lasers, in general. The periodicity of the oscillations, denoted τ, is a function of the pump power and data obtained for pump powers as large as 2.4 $P_{\rm th}$ (for 1% cavity output coupling) are shown in Fig. 12. Note that τ decreases linearly with increasing pump power and that the spiking period is roughly what one would expect for the buildup time for the $^5S_2$ population. Assuming: 1) the pumping intensity in the fiber core to be $\approx 10^5$ W-cm^{-2} and, 2) the time for the buildup of population in the upper laser level resulting from single photon transitions from the $^5I_6$ and $^5I_7$ states to be ~ 10 μs ($P \sim 2 \cdot P_{\rm th}$, Fig. 11), then the effective cross-section σ for the second stage of the pumping process is $\sim 3 \cdot 10^{-19}$ cm^2. In short, the dependence of τ on pump power is *consistent* with the expected pumping rate for the upper laser level. Consequently, we attribute the quasi-CW operation of the laser to self Q-switching which is a result of saturable loss in the active medium arising from ground state absorption. A magnified view of the early portion of the laser waveform observed when the pump beam is chopped (Fig. 13) shows the turn-on transient for the laser ($L = 22$ cm) to be ~ 300 μs (varies by $\pm 10\%$ from pulse-to-pulse).

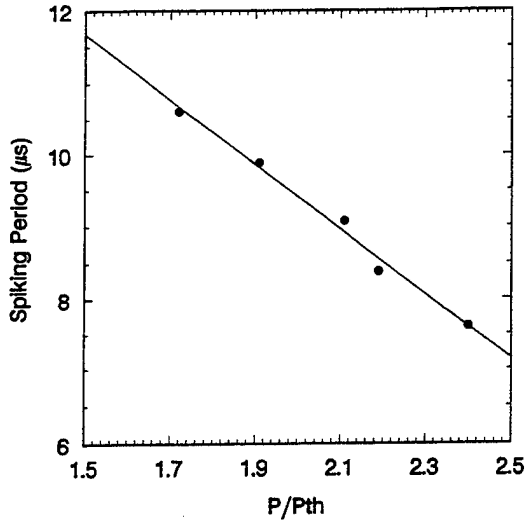

Fig. 12. Variation of the laser output spiking period with the pump power at 643 nm for a cavity output coupling of 1%. $P_{\rm th}$ is the threshold pumping power (120 mW incident on input coupling optics). The solid line represents the least-squares fit to the data.

IV. Summary and Conclusions

The output power and temporal and tuning behavior of the green (~549 nm) Ho:ZBLAN fiber laser has been studied for fibers ranging in length from ~20 to 86 cm. Output powers exceeding 38 mW have been measured for 280 mW of absorbed pump power and 30% cavity output coupling. For the highest output coupling studied to date (30%), the slope efficiency of the laser with respect to absorbed power is 24% for a multimode (11 μm core) fiber. Since the output power has not yet saturated with respect to either output coupling or pump power, it is likely that considerably higher output powers

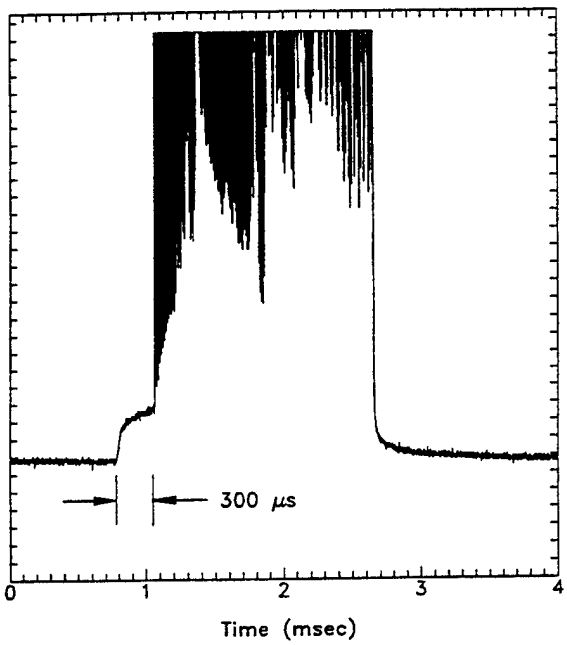

Fig. 13. Expanded view of the early portion of the Ho^{3+} laser waveform recorded when the pump beam is chopped.

and efficiencies will be realized with larger output couplings. Furthermore, the high NA (>0.3), single mode fibers that are currently available will undoubtedly yield considerably lower pump power thresholds than those reported here.

With two prisms installed in the optical cavity, the Ho fiber laser has been line-tuned over a ~11 nm region in the green. Although the laser currently operates in a self-pulsing mode, it appears that, in a manner similar to that observed for the Tm:ZBLAN transition at 455 nm [23], the green Ho:ZBLAN laser is capable of true CW operation with an alternate pumping scheme.

The role of the depletion of ground state population on laser performance is evident in the laser spectrum and conversion efficiency of the device. Because of ground state absorption losses, an ideal three-level laser is an inherently inefficient device. However, the behavior of the Ho:ZBLAN fiber laser reported previously [2], [7], [8] as well as the results described earlier demonstrate that this laser is a quasi-3 level system in which strong depletion of the ground state can occur because of the presence of intermediate levels—namely, the $^5I_6$ and $^5I_7$ states of Ho^{3+}. Their ability to store energy drives the behavior of the Ho:ZBLAN laser toward that of a four-level system.

Finally, by measuring the laser output power from the 21 cm long fiber as a function of cavity output coupling for the pump power fixed at 250 mW (threshold pump power for 20% output coupling), the small signal gain coefficient at 550 nm is estimated to be 0.9%-cm^{-1} for $P = 320$ mW. For the sake of comparison, it should be noted that the small signal gain coefficient for the blue-green (491 nm) and red (635 nm) lasing transitions in Pr:ZBLAN fiber have been estimated by Tropper *et al.* [24] to be ~0.2%-cm^{-1} and 2.7%-cm^{-1}, respectively. The latter is the highest gain visible upconversion laser demonstrated to date; in fact, the 635 nm line lases when the 4% reflection from one end of the cleaved fiber serves as the output coupler for the optical cavity. Consequently, the estimated small signal gain coefficient for Ho:ZBLAN is intermediate to those for two well-known lasing transitions of the Pr^{3+} ion and is within a factor of three for the gain measured for the 635 nm line.

The slope efficiency and wide tunability of this fiber laser make it an attractive source for applications requiring green radiation, and the recent availability of red ($\lambda \sim 640$ nm) laser diodes suggests that a compact version of this fiber laser will be developed in the near future.

ACKNOWLEDGMENT

The authors gratefully acknowledge the technical assistance of J. L. Sexton and J. W. Carlson.

REFERENCES

[1] J. Y. Allain, M. Monerie, and H. Poignant, "Blue upconversion fluorozirconate fiber laser," *Electron. Lett.*, vol. 26, pp. 166–168, 1990.
[2] ——, "Room temperature CW tunable green upconversion holmium fiber laser," *Electron. Lett.*, vol. 24, pp. 261–263, 1990.
[3] D. S. Funk, J. W. Carlson, and J. G. Eden, "Ultraviolet (381 nm), room temperature laser in neodymium-doped fluorozirconate fiber," *Electron. Lett.*, vol. 30, pp. 1859–1860, 1994.
[4] ——, "Room temperature fluorozirconate glass fiber laser in the violet (412 nm)," *Opt. Lett.*, vol. 20, pp. 1474–1476, 1995.
[5] D. S. Funk and J. G. Eden, "Glass fiber lasers in the ultraviolet and visible," *J. Select. Topics Quantum Electron.*, vol. 1, pp. 784–791, 1995.
[6] S. G. Grubb, private communication.
[7] J. Y. Allain, M. Monerie, and H. Poignant, "Characteristics and dynamics of a room temperature CW tunable green upconversion holmium fiber laser," in *Proc. 16th European Conf. Opt. Commun. (ECOC '90)*, 1990, vol. 1, pp. 575–578.
[8] D. S. Funk, S. B. Stevens, and J. G. Eden, "Excitation spectra of the green Ho:fluorozirconate glass fiber laser," *IEEE Photon. Technol. Lett.*, vol. 5, pp. 154–157, 1993.
[9] Y. K. Voron'ko, A. A. Kaminskii, V. V. Osiko, and A. M. Prokhorov, "Stimulated emission of Ho^{3+} in CaF_2 at $\lambda = 5512$ Å," *Zh. Eksp. Teor. Fiz. Pis'ma Red.*, vol. 1, pp. 5–9, 1965; *JETP Lett.*, vol. 1, pp. 3–5, 1965.
[10] L. F. Johnson and H. J. Guggenheim, "Infrared-pumped visible laser," *Appl. Phys. Lett.*, vol. 19, pp. 44–47, 1971.
[11] D. S. Funk, S. B. Stevens, S. S. Wu, and J. G. Eden, "Characterization and modeling of the holmium upconversion fiber laser," in *Proc. SPIE*, 1994, vol. 2115, pp. 40–44.
[12] M. D. Shinn, W. A. Sibley, M. G. Drexhage, and R. N. Brown, "Optical transitions of Er^{3+} ions in fluorozirconate glass," *Phys. Rev. B*, vol. 27, pp. 6635–6648, 1983.
[13] K. Tanimura, M. D. Shinn, W. A. Sibley, M. G. Drexhage, and R. N. Brown, "Optical transitions of Ho^{3+} ions in fluorozirconate glass," *Phys. Rev. B*, vol. 30, pp. 2429–2437, 1984.
[14] R. Reisfeld and C. K. Jorgensen, *Excited State Phenomena in Vitreous Materials*. Amsterdam, The Netherlands: Elsevier, 1987, pp. 1–90.
[15] R. Reisfeld, M. Eyal, E. Greenberg, and C. K. Jørgensen, "Luminescence of six *J*-levels of holmium (III) in barium zirconium fluoride glass at room temperature," *Chem. Phys. Lett.*, vol. 118, pp. 25–28, 1985.
[16] F. Gan and H. Zheng, "Spectral properties of Ho^{3+} ions in noncrystalline fluorides," *J. Non-Cryst. Solids*, vols. 95 and 96, pp. 771–776, 1987.
[17] J. B. Gruber, M. E. Hills, M. D. Seltzer, S. B. Stevens, C. A. Morrison, G. A. Turner, and M. R. Kokta, "Energy levels and crystal quantum states of trivalent holmium in yttrium aluminum garnet," *J. Appl. Phys.*, vol. 69, pp. 8183–8204, 1991.
[18] F. Tong, W. P. Risk, R. M. Macfarlane, and W. Lenth, "551 nm diode laser-pumped upconversion laser," *Electron. Lett.*, vol. 25, pp. 1389–1391, 1989.
[19] R. A. McFarlane, "Dual wavelength visible upconversion laser," *Appl. Phys. Lett.*, vol. 54, pp. 2301–2302, 1989.
[20] T. Herbert, W. P. Risk, R. M. Macfarlane, and W. Lenth, "Diode laser pumped 551 nm upconversion laser in $YLiF_4:Er^{3+}$," *Proc. Opt. Soc.*

Am. - Solid-State Lasers, H. P. Jenssen and G. Dubé, Eds., Washington, DC, Optical Society of America, 1990, vol. 6, pp. 379–383.
[21] F. Heine, E. Heumann, T. Danger, T. Schweizer, G. Huber, and B. Chai, "Green upconversion continuous wave Er^{3+}: $LiYF_4$ laser at room temperature," *Appl. Phys. Lett.*, vol. 65, pp. 383–384, 1994.
[22] F. Sanchez, P. LeBoudec, P.-L. François, and G. Stephan, "Effects of ion pairs on the dynamics of erbium-doped fiber lasers," *Phys. Rev. A*, vol. 48, pp. 2220–2229, 1993.
[23] M. P. LeFlohic, J. Y. Allain, G. M. Stéphan, and G. Mazé, "Room temperature continuous wave upconversion laser at 455 nm in a Tm^{3+} fluorozirconate fiber," *Opt. Lett.*, vol. 19, pp. 1982–1984, 1994.
[24] A. C. Tropper, J. N. Carter, R. D. T. Lauder, D. C. Hanna, S. T. Davey, and D. Szebesta, "Analysis of blue and red laser performance of the infrared-pumped praseodymium-doped fluoride fiber laser," *J. Opt. Soc. Am. B*, vol. 11, pp. 886–893, 1994.

David S. Funk received the B.S. degree in physics from the University of Puget Sound, Tacoma, WA, in 1989.

He is currently a graduate student in the Department of Physics at the University of Illinois, Urbana. His research interests include the study of rare earth-doped optical fiber and waveguide devices, and nonlinear optical waveguides.

S. B. Stevens, photograph and biography not available at the time of publication.

S. S. Wu, photograph and biography not available at the time of publication.

J. Gary Eden (S'75–M'76–SM'82–F'88) received the B.S. degree in electrical engineering from the University of Maryland, College Park, and the M.S. and Ph.D. degrees from the University of Illinois in 1973, and 1976, respectively.

He was awarded a National Research Council Postdoctoral Research Associateship from the Naval Research Laboratory, Washington, DC, in 1975. Subsequently, he joined the staff of the Laser Physics Branch of the NRL and, during his tenure there, made several contributions to the areas of visible and ultraviolet lasers and gas laser spectroscopy, including co-discovery of the KrCl laser (222 nm) and the optically pumped HgCl and XeF lasers. Since 1979, he has been a member of the faculty of the Department of Electrical and Computer Engineering at the University of Illinois, Urbana. He is also a member of the graduate faculty in physics and currently serves as Associate Dean of the graduate college. His research group has demonstrated several new molecular lasers and amplifiers in the visible and near-IR (including CdI, ZnI and I_2 (500 nm)) and developed laser spectroscopic techniques for studying the Rydberg and autoionizing states of diatomic and triatomic molecules. Results in the latter area include rotationally resolving Rydberg-Rydberg transitions of the rare gas dimers (Ne_2, Ar_2) and the spectroscopy of rare gas-halide molecules by photoassociation. He has also carried out extensive research on the growth of semiconductor and metal films by photochemical processes in the gas phase. His current research interests focus on upconversion lasers in waveguides and ultrafast, nonlinear techniques for generating coherent VUV radiation. He has published more than 130 papers, is the author of one book, and has been granted 12 patents.

Dr. Eden is Fellow of the IEEE, the American Physical Society, and the Optical Society of America. He recently served (1993–1995) as the Vice-President for Technical Affairs of the IEEE Lasers and Electro-Optics Society (LEOS) and is Editor of the LEOS book series *Progress in Lasers and Electro-Optics*.